

## Accepted Manuscript

Stable isotope ( $\delta^{18}\text{O}$  and  $\delta^{13}\text{C}$ ) sclerochronology of Callovian (Middle Jurassic) bivalves (*Gryphaea (Bilobissa) dilobotes*) and belemnites (*Cylindroteuthis puzosiana*) from the Peterborough Member of the Oxford Clay Formation (Cambridgeshire, England): evidence of palaeoclimate, water depth and belemnite behaviour

C. Mettam, A.L.A. Johnson, E.V. Nunn, B.R. Schöne

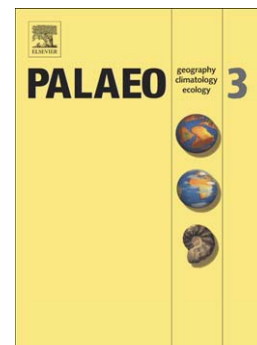
PII: S0031-0182(14)00020-0  
DOI: doi: [10.1016/j.palaeo.2014.01.010](https://doi.org/10.1016/j.palaeo.2014.01.010)  
Reference: PALAEO 6728

To appear in: *Palaeogeography, Palaeoclimatology, Palaeoecology*

Received date: 10 August 2013  
Revised date: 27 December 2013  
Accepted date: 18 January 2014

Please cite this article as: Mettam, C., Johnson, A.L.A., Nunn, E.V., Schöne, B.R., Stable isotope ( $\delta^{18}\text{O}$  and  $\delta^{13}\text{C}$ ) sclerochronology of Callovian (Middle Jurassic) bivalves (*Gryphaea (Bilobissa) dilobotes*) and belemnites (*Cylindroteuthis puzosiana*) from the Peterborough Member of the Oxford Clay Formation (Cambridgeshire, England): evidence of palaeoclimate, water depth and belemnite behaviour, *Palaeogeography, Palaeoclimatology, Palaeoecology* (2014), doi: [10.1016/j.palaeo.2014.01.010](https://doi.org/10.1016/j.palaeo.2014.01.010)

This is a PDF file of an unedited manuscript that has been accepted for publication. As a service to our customers we are providing this early version of the manuscript. The manuscript will undergo copyediting, typesetting, and review of the resulting proof before it is published in its final form. Please note that during the production process errors may be discovered which could affect the content, and all legal disclaimers that apply to the journal pertain.



**Stable isotope ( $\delta^{18}\text{O}$  and  $\delta^{13}\text{C}$ ) sclerochronology of Callovian (Middle Jurassic) bivalves (*Gryphaea (Bilobissa) dilobotes*) and belemnites (*Cylindroteuthis puzosiana*) from the Peterborough Member of the Oxford Clay Formation (Cambridgeshire, England): evidence of palaeoclimate, water depth and belemnite behaviour**

Mettam, C<sup>a\*</sup>, Johnson, ALA<sup>a</sup>, Nunn, EV<sup>b</sup>, Schöne, BR<sup>b</sup>

<sup>a</sup> Geographical, Earth and Environmental Sciences, School of Science, University of Derby, Derby, DE22 1GB, UK

<sup>b</sup> Institute of Geosciences, University of Mainz, 55128 Mainz, Germany

\*corresponding author: C.Mettam1@unimail.derby.ac.uk

Tel: +44 (0)1782 782371

**Abstract**

Incremental  $\delta^{18}\text{O}$  and  $\delta^{13}\text{C}$  signals were obtained from three well-preserved specimens of *Cylindroteuthis puzosiana* and from three well-preserved specimens of *Gryphaea (Bilobissa) dilobotes* from the Peterborough Member of the Oxford Clay Formation (Cambridgeshire, England). Through-ontogeny (sclerochronological)  $\delta^{18}\text{O}$  data from *G. (B.) dilobotes* appear to faithfully record seasonal temperature variations in benthic Callovian waters of the study area, which range from c.14°C to c. 17°C (arithmetic mean temperature c. 15°C). Water depth is estimated to have been in the region of c. 50m, based upon comparisons between these data, previously published non-incremental sea surface  $\delta^{18}\text{O}$  values, and a modern analogue situation. Productivity in Callovian waters was comparable with that in modern seas, based upon  $\delta^{13}\text{C}$  data from *G. (B.) dilobotes*, with  $^{13}\text{C}$  depletion occurring during warmer periods, possibly related to an interaction between plankton blooms and intra-annual variations in mixing across a thermocline. Incremental  $\delta^{18}\text{O}$  data from *C. puzosiana* provide temperature minima of c. 11°C for all specimens but with maxima varying between c. 14°C and c. 16°C for different individuals (arithmetic mean values c. 13°C). Temperatures for late ontogeny, when

the *C. puzosiana* individuals must have been living close to the study site and hence the analysed specimens of *G. (B.) dilobotes*, are closely comparable to those indicated by the latter. However, for significant portions of ontogeny *C. puzosiana* experienced temperatures between *c.* 2°C and *c.* 3°C cooler than the winter minimum as recorded by co-occurring *G. (B.) dilobotes*. Comparisons with modern seas suggest that descent to a depth of *c.* 1000m would be necessary to explain such cool minimum temperatures. This can be discounted due to the lack of deep waters locally and due to estimates of the depth tolerance of belemnites. The most likely cause of cool  $\delta^{18}\text{O}$  signals from *C. puzosiana* is a cosmopolitan lifestyle including migration to more northerly latitudes. Mean  $\delta^{13}\text{C}$  values from *C. puzosiana* are comparable with those from *G. (B.) dilobotes*. However, the incrementally acquired data are highly variable and probably influenced by metabolic effects. The probable identification of migratory behaviour in *C. puzosiana* calls into question the reliability of some belemnite species as place-specific palaeoenvironmental archives and highlights the benefits of adopting a sclerochronological approach.

### Keywords

Jurassic; Paleoseasonality; *Gryphaea*; Belemnite; Oxygen and carbon stable isotopes; Sclerochronology

## 1. Introduction

Belemnite rostra have been widely used as a source of stable oxygen ( $\delta^{18}\text{O}$ ) and carbon ( $\delta^{13}\text{C}$ ) isotope signals for the reconstruction of Mesozoic climatic and oceanographic conditions (e.g. Price et al., 2000; Price and Mutterlose, 2004; Nunn et al., 2009; Wierzbowski and Joachimski, 2009; Nunn and Price, 2010; Price, 2010; Price et al., 2011; Price et al., 2012; Alberti et al., 2012). This is because (1) they are widely considered to record oxygen isotope ratios in equilibrium with ambient oceanic water, although there are suspicions that metabolic effects may influence carbon isotopes (Wierzbowski, 2004; McArthur et al., 2007; Price and Page, 2008; Žák et al., 2011), and (2) their robust form and low-magnesium calcite composition is believed to be resistant to diagenesis, thus preserving original isotope ratios (Rosales et al., 2004; Wierzbowski and Joachimski, 2009; Price et al., 2012).

Despite their apparent suitability, there have been some concerns regarding the utilization of data from belemnites when reconstructing environmental evolution through geological time. This is because firstly, signals are likely to be obtained from different assemblages of belemnite species at different geological times, and could therefore represent different ecological niches and lifestyles (McArthur et al., 2007; Li et al., 2012) and secondly, and central to this paper, because research indicates that in some instances, belemnites provide cooler than expected oxygen isotope palaeotemperatures when compared to other contemporary proxies (e.g. Anderson et al., 1994; Voigt et al., 2003; Bodin et al., 2009; Dera et al., 2009; Mutterlose et al., 2010; Mutterlose et al., 2012). This phenomenon may be caused by some species following cosmopolitan lifestyles, with significant time spent at higher latitudes. This would present as a positive (cooler) shift in  $\delta^{18}\text{O}$  values when such data are

generated from homogenised samples or samples from randomly located points within the rostra.

Extensive migration to cooler waters at a significant distance from the site of collection was recently proposed by Alberti et al. (2012) to explain why Jurassic belemnites from the Kachchh Basin returned cooler  $\delta^{18}\text{O}$  palaeotemperatures than local brachiopods and oysters because the cool belemnite palaeotemperatures could not be accounted for by local depth variations. However, whilst this argument is logical, more robust evidence is required in order to confirm this hypothesis. Should such evidence become available it may help elucidate the nature of belemnite behaviour: whether belemnites were nektonic or nekto-benthic, whether they lived in open oceanic or neritic settings, to what extent they migrated on a daily and seasonal basis, and whether patterns of behaviour varied between species (Doyle and Macdonald, 1993; Price and Sellwood, 1997; Rosales et al., 2004; Price and Page, 2008).

Possibly the best method of exploring belemnite behaviour in this context is to apply a sclerochronological approach to the collection of  $\delta^{18}\text{O}$  data. If the belemnite species investigated stayed within a restricted ecological niche during its lifetime, then through-ontogeny palaeotemperatures calculated from incremental  $\delta^{18}\text{O}$  signals should, at no time, yield palaeotemperatures significantly outside of the range of those determined from an equivalent analysis of a non-migratory organism collected from the same locality and horizon. If the belemnite were to provide evidence of unexpectedly cool or warm temperatures, then this might indeed be indicative of migratory habits, and furthermore, would suggest that only rostrum material deposited during the latest stages of ontogeny accurately represents local conditions.

Previous studies of the Jurassic belemnite *Cylindroteuthis puzosiana* from the Peterborough Member of the Oxford Clay Formation of England have yielded average oxygen isotope palaeotemperatures that were unexpectedly cool in comparison with those derived from other local proxies including *Gryphaea* sp. (Anderson et al., 1994). However, whether these cool palaeotemperatures were due to *C. puzosiana* occupying a nekto-benthic niche in waters deeper than those at the collection site or whether they were due to migration to cooler bodies of water remains unclear. In order to clarify the life habits of *C. puzosiana* sclerochronological investigations were undertaken to explore intra-rostrum variations in stable oxygen and carbon isotope signals. The findings were then compared with through-ontogeny stable oxygen and carbon isotope signals from *Gryphaea (Bilobissa) dilobotes*, a coeval, benthic bivalve that would be expected to deliver trustworthy data on temperature variation on the seabed at the collection site due to its sessile mode of life.

## **2. Geological setting**

### *2.1. Oxford Clay Formation*

Outcropping from Yorkshire, through the East Midlands and to Dorset on the south coast of England (Fig.1), the Oxford Clay has three argillaceous sub-units, of which the Peterborough Member is the lowest. This organic-rich, sometimes fissile sub-unit, which is absent north of the Humber, is some 15 to 20m thick at Whittlesey (near Peterborough, Cambridgeshire), the nearest settlement to the site of specimen collection, and the stratigraphy in the lower part of this sub-unit (the stratigraphic horizons from which specimens were collected – see sections 2.3 and 3.1) remains uniform throughout the Peterborough area. The Peterborough Member lies conformably on top of the sandy Kellaways Formation, whilst above, the Stewartby

Member of the Oxford Clay Formation represents a change to less organic, blockier mudstone (Duff, 1978; Page, 1989; Hudson et al., 1991).

**Fig. 1. Outcrops of the Oxford Clay in England and specimen collection site.**

**Map modified after Hudson and Martill (1994), areas of outcrop shown by shaded area and asterisk indicating site of collection**

## *2.2. Palaeogeography*

The Peterborough Member was deposited during the Callovian (Middle Jurassic) in an epeiric sea, at a palaeolatitude of approximately 35° north. Sedimentological and palaeontological evidence indicates that the location of modern Whittlesey would have been at most a few tens of kilometres from the Anglo-Brabant Platform (Fig. 2). Sediment input included terrestrial detritus, phytoplanktonic material, marine and land macro-organisms and woody debris (Hudson, 1978; Page, 1989; Belin and Kenig, 1994; Hudson and Martill, 1994; Norry et al., 1994; Hudson et al., 1991). Waters in the area were less than 50m deep for at least 150km from the shore (Hudson and Martill, 1991) and to the south, these waters were connected to the Tethys Ocean, whilst to the north there were connections to Boreal waters between the Mid North Sea High/Scottish Landmass and the Irish Landmass, and through the Rockall/Faeroe Rift and the Hebridean and North Minch Basins (Fig. 2). Some of these marine conduits were related to Jurassic rifting and may explain the spread of Boreal ammonites towards the Tethys Ocean, and Tethyan species towards the Boreal Realm at this time (Ziegler, 1990; Bradshaw et al., 1992; Hudson and Martill, 1994).

**Fig. 2. The Palaeogeography of North-West Europe in the Callovian**

**Palaeogeographic map modified after Bradshaw et al. (1992), asterisk indicates site of collection of specimens**

### *2.3. Palaeoenvironment*

Previous studies using  $\delta^{18}\text{O}$  data from supposedly pendant bivalves and ammonites from the Oxford Clay Formation have established average sea surface temperatures (SSTs) of 19°C to 21°C for the UK at this time (Hudson, 1978; Anderson et al., 1994), conditions comparable with the modern Gulf of Tunis at similar latitudes (Johnson et al., 2009). These data support palaeobotanical and sedimentological interpretations which suggest that the UK climate evolved throughout the Middle Jurassic as warm temperate conditions gave way to a Mediterranean-like climate, characterised by mild, wet winters and dry summers by the early Bathonian, with a subsequent trend towards increasing aridity (Morgans, 1999, Morgans et al., 1999). These conditions were within the context of a global greenhouse with weakly defined climatic zones (Frakes et al., 1992; Sellwood and Valdes, 1997; Poulsen and Riding, 2003; Brigaud et al., 2008).

Whilst fossil evidence indicates that surface and near-surface waters supported a diverse marine ecosystem during the deposition of the Peterborough Member, it has been argued that benthic life may have been periodically restricted by low oxygen levels (Hudson et al., 1991; Belin and Kenig, 1994; Hudson and Martill, 1994; Macquaker, 1994; Martill et al., 1994; Kenig et al., 2004). Lower horizons within the Peterborough Member show such changes particularly well, with organic-rich shales, such as bed 10, deposited when the seabed was possibly euxinic, and shell beds, such as beds 9 and 11 (Fig. 3), suggesting periods of increased aeration. Bed 10 does display flattened, greenish burrows in its upper laminae, but

these indicate burrowing organisms penetrating the substrate from above during later oxygenated periods.

**Fig. 3. Stratigraphy of the lower part of the Peterborough Member in the Peterborough area.**

**Diagram modified after Hudson and Martill (1994b).**

#### *2.4. Preservation of fossil material*

The Oxford Clay Formation is well documented for yielding well preserved fossils, including the organic remains of fish and coleoids at the now inaccessible Lagerstätte at Christian Malford and more recently from a site at Ashton Keynes, both in Wiltshire (Wilby et al., 2004). Whilst such soft-body specimens have not been recovered from the Whittlesey area, preservation of fossil material, sometimes including aragonite, is still considered to be excellent (Hudson and Martill, 1991). A number of factors may have contributed to this level of good preservation. These include deposition during periods of anoxia, which would have precluded biological action, and the fine grained matrix, which would have limited permeation of potential diagenetic fluids after burial. Moderate overburden restricted burial temperatures to probably no more than 50°C and also limited vertical compressive forces, whilst lateral tectonic pressures in the post-Jurassic Midlands were minimal (Hudson, 1978; Hudson et al., 1991; Hudson and Martill, 1994; Kenig et al., 1994; 2004; Macquaker, 1994).

### **3. Materials and methods**

#### *3.1. Field sites*

Specimens of *C. puzosiana* and *G. (B.) dilobotes* were collected for later screening from Bradley Fen Quarry, Whittlesey (National Grid Reference TL 228 977) in May 2010 and from Must Farm Quarry, Whittlesey (National Grid Reference TL 232 968) in September 2011. The close proximity of all specimens suggests that they would have died in this locality, as the lack of any sedimentary structures in the Peterborough member argues against sediment transport.

At both collection sites, bed 10 acts as a reference horizon for collection as it is left intact (since its top marks the base of viable clay workings) and it is easily identifiable due to the presence of large calcareous concretions and a fissile fabric. At Bradley Fen specimens were collected from bed 11 in the *Kosmoceras (Gulielmiceras) jason* ammonite subzone. This is a coarser grained horizon than bed 10, with abundant *G. (B.) dilobotes* and *C. puzosiana*. At Must Farm, the small area that was safely accessible in the new workings meant exposures of bed 11 were both extremely limited and badly damaged due to the movement of quarry machinery. However, it was possible to collect from a lower coarse grained *Gryphaea* shell bed (bed 9) in the *Kosmoceras (Gulielmiceras) medea* ammonite subzone which was accessible by excavating through bed 10 (approximately 15 to 20cm thick).

### 3.2. Screening

All specimens were gently cleaned in water to remove sediment. Initial selection of specimens for further analysis was undertaken by visual inspection with any specimens of either taxon displaying damage being rejected. Belemnites were selected for further examination based on macro-scale visible characteristics (see 4.1). Those specimens chosen for further examination were cleaned again in order to eliminate organic material. This involved bathing

in warm 5% NaOCl solution followed by a 96% ethanol bath. Specimens were then washed in distilled water and dried for 12 hours at 60°C (see Heilmayer et al., 2004 for full methodology).

Tests for diagenetic alteration were undertaken in order to eliminate the possibility of primary isotopic signals being overwritten. Carbonate stains were used to test for the replacement of non-ferroan with ferroan calcite. This process involved slides being initially etched with 1.5% HCl (10-15 sec), then stained by immersion in potassium ferricyanide and alizarin red-S mixed in HCl (30-45 sec), followed by a final stain in alizarin red-S mixed in HCl (10-15 sec) (see Dickson, 1965 for full methodology).

Cathodoluminescence (CL) testing was also employed in order to identify the presence of manganese in calcite, which is another common diagenetic element (Price and Sellwood, 1997; Rosales et al., 2001; Rosales et al., 2004). This involved bombarding an uncovered thick section (approximately 100µm thick) with cathode rays in a vacuum chamber to induce luminescence, with the gun current set at 450µA and a voltage of ~10kV. It is essential that carbonate staining is done in tandem with CL, as the presence of iron is known to inhibit luminescence (Price and Nunn 2010; Tomašových and Farkaš, 2005). In both instances images were captured using a digital camera mounted upon an optical microscope. In order to detect any non-calcareous phases, an uncovered thick section (100µm) of each specimen was also examined via back scattered electron microscopy (BSEM), with an acceleration voltage of 20kV.

### 3.3. *Sampling and analysis*

After screening for potential alteration three specimens of each taxon were selected for sampling. Two *Gryphaea* and two belemnites were selected from the *jason* ammonite subzone and one of each taxon from the *medea* subzone.

In order to sample carbonate from *Gryphaea* the procedure of Schöne et al. (2005) was followed. First, a 3mm thick slab was cut from the umbo to the ventral margin of the left valve of each specimen. The slabs were mounted on slides using epoxy glue and the cut surfaces polished and photographed under a microscope to create a large composite image. The *Gryphaea* were drilled immediately beneath the outer shell surface under a microscope using a dental drill, beginning at the umbo and moving towards the ventral margin to create an ontogenetic series of samples, with earliest life nearest the umbo (Fig. 4). Sample points were placed as close together as possible without them merging into each other; this meant a distance of 2 to 2.5mm between the centres of each sample point. The distance from the umbo of sample points was measured from the point of the umbo to the sample point (Fig. 4). Although some species of *Gryphaea* are considered to live for up to 17 years (Jones and Gould, 1999) , those in the Peterborough Member shell beds are not considered to exceed ~10 years of age (Kenig et al. 2004). Data for all specimens comes from the earliest ontogeny (years 1 to 2) where the shell is most robust. Further towards the ventral margin the shell becomes more fragile and crumbles when drilled and CL and carbonate staining reveal that this portion of the shell is more prone to alteration.

**Fig. 4. Sampling of *G. (B.) dilobotes* and measurement of distance from umbo**

In order to systematically sample belemnite carbonate through ontogeny it is important to consider their mode of growth. It is believed that the growth of belemnite rostra is initiated at the protoconch, and that calcite is added by simultaneous accretion over the outer surface of the rostrum. Consequently, each period of carbonate addition replicates the entire structure, and therefore the surface of the rostrum represents an ontogenetically equivalent calcite layer (O'Neill et al., 2003). The precipitated calcite crystals form a radial pattern centred on the apical region and these structures are cross cut by growth increments separated by darker growth rings, which are believed to reflect reductions in the rate of accretion of calcite onto the rostrum. Whilst the precise nature and periodicity of their formation is uncertain (Dunca et al., 2006; Wierzbowski and Joachimski, 2009), these increments clearly mark increasing age as the rostrum edge is approached and thus provide a basis for extracting an ontogenetic series of samples.

A 3mm thick slab was cut across each belemnite, perpendicular to its long axis, at the point of greatest rostrum circumference, just below the alveolar region. By cutting the belemnites here, just below the phragmocone, it was possible to ensure that the dorsoventral cross-sections were as wide and ontogenetically complete as possible. Whilst some of the earliest growth increments may not be represented in these sections (since the presence of cracks meant that it was not always possible to take samples immediately adjacent to the protoconch), all other growth stages (preservation permitting) are represented.

This slab was then mounted onto a slide and polished so that growth increments could be clearly seen. A 3mm wide strip, containing the apical region, was then cut from each slab (Fig. 5). This species of belemnite has an asymmetrical rostrum (Li and McArthur, 2013), with

the longer radius of the rostrum towards the dorsal margin, as a result of the apical region being offset towards to the venter. It would have been desirable to cut the slabs across the maximum radius (vertically from apical region to dorsal margin), and thus take advantage of the portion of rostrum offering the highest possible resolution. However, this would in all cases have resulted in inclusion of slightly damaged (potentially altered) material. Hence, all strips were cut to include the apical canal but at various angles to the maximum diameter in order to avoid minor cracks. The resulting sections were then remounted on slides and photographed to create a composite image.

Sampling was undertaken using a dental burr mounted under a microscope. Material was milled away, starting from the exterior, to generate samples of carbonate powder from arcs parallel to growth rings (Fig. 5).

**Fig. 5. Sampling of *C. puzosiana***

**(A, position from which slabs were cut. B, how samples were milled in relation to age)**

Specimens G1 and G2 were drilled, and C1 and C2 milled, at the Institute of Geosciences, University of Mainz, Germany, whilst specimen G3 was drilled and C3 milled at the School of Science, University of Derby, UK. All samples were analysed at the Institute of Geosciences, University of Mainz, Germany, on a Thermo Finnigan MAT 253 continuous flow isotope ratio mass spectrometer, equipped with a Gas Bench II. Isotope data were calibrated against Carrara marble standard ( $\delta^{18}\text{O} = -1.74\text{‰}$ ;  $\delta^{13}\text{C} = 2.01\text{‰}$ ) with  $1\sigma$  external reproducibility and internal precision of  $0.07\text{‰}$  and  $0.03\text{‰}$  for oxygen and carbon isotope values respectively.

Results are expressed in parts per thousand with respect to Vienna Pee Dee belemnite standard (‰ V-PDB).

### 3.4. $\delta^{18}\text{O}$ data and palaeotemperatures

The  $\delta^{18}\text{O}$  palaeotemperatures for both *G. (B.) dilobotes* and *C. puzosiana* were calculated using the equation of Anderson and Arthur (1983):

$$T(^{\circ}\text{C}) = 16.0 - 4.14 (\delta^{18}\text{O}_{\text{calcite}} - \delta^{18}\text{O}_{\text{seawater}}) + 0.13 (\delta^{18}\text{O}_{\text{calcite}} - \delta^{18}\text{O}_{\text{seawater}})^2 \quad (1)$$

with an adjustment made to  $\delta^{18}\text{O}_{\text{seawater}}$  of -1‰ as used by other authors, based on the lack of polar ice in the Jurassic (Frakes, 1979; Sellwood and Valdes, 1997; Poulsen and Riding, 2003; Frakes et al., 1992; Price and Sellwood, 1997).

### 3.5. Presentation of data

The  $\delta^{18}\text{O}$  and  $\delta^{13}\text{C}$  data for each specimen are presented in Fig. 6. The oxygen isotope axis is reversed in order that lower values of  $\delta^{18}\text{O}$ , indicating warmer temperatures, plot towards the top. Data for specimens of *G. (B.) dilobotes* are shown in Table 1 and for *C. puzosiana* in Table 2.

## 4. Results

### 4.1. Preservation

The specimens chosen for sampling were all considered to be well-preserved based upon a range of criteria including visual inspection, carbonate staining, CL and BSEM.

The *G. (B.) dilobotes* specimens were inspected for cracks which might have provided a pathway for the penetration of diagenetic fluids. Whilst cracks were visible, those *G. (B.) dilobotes* specimens selected for further testing had significant undamaged portions extending from the umbo towards the ventral margin, indicating the possibility of extracting an acceptable number of unaltered samples. Specimens of *C. puzosiana* from the *Kosmoceras (Gulielmiceras) jason* ammonite subzone were honey coloured and translucent, with a radial crystalline structure and visible growth increments, all evidence suggesting good preservation (Nunn and Price, 2010; Price and Rogov, 2009; Price, 2010; McArthur et al., 2007). Further positive indications came from specimen C1 which was retrieved with a portion of the aragonite phragmocone intact. Belemnite specimens from the *Kosmoceras (Gulielmiceras) medea* ammonite subzone were all darker and less translucent than specimens from the *jason* subzone. Specimen C3 was eventually selected as the best preserved belemnite from this horizon based upon the examinations described below, although cracks in the area close to the apical region had to be avoided during sampling.

Testing via CL for the presence of manganese suggested that all specimens from the *jason* subzone were well preserved, displaying predominantly blue luminescence. Dull red luminescence was restricted to faint bands in *G. (B.) dilobotes* and does not necessarily signify alteration as similar features are noted in modern bivalves and brachiopods (Tomašových and Farkaš, 2005; Lartaud et al., 2010). Barbin et al. (1991), who utilized hot CL analysis, argue that such structures, which represent variations in manganese content, may be due to differential growth rates in a chemically stable environment or to cyclical changes in the chemical composition of the ambient waters. An alternative view with regard to these features in Jurassic oysters from Wierzbowski and Joachimski (2007) is that

luminescent bands may represent sediment trapped within growth increments. Similar dull red banding was present in a restricted number of growth rings in *C. puzosiana*, but again is not necessarily indicative of alteration as this is a feature also identified in modern cephalopods (Barbin et al., 1994; Wierzbowski, 2004). Bright orange/red luminescence in specimens of both taxa from the *jason* subzone was restricted to large cracks and material attached to the exterior, areas that were easily avoided during sampling. Specimens from the *medea* subzone revealed less promising CL results, lacking blue colouration and with bright orange/red in cracks for both taxa and also in some growth rings for *C. puzosiana*.

Carbonate staining provided encouraging results, with all specimens showing predominantly pink colouration (indicative of unaltered calcite) and with strong blue colouration (indicating the replacement of calcium by iron) restricted to easily avoidable cracks and surface material. Specimens from the *medea* subzone did display some faint blue colouration, especially adjacent to the outer surface of the shell in *G. (B.) dilobotes* (G3) and at the rostrum edge in *C. puzosiana* (C3).

BSEM revealed that all specimens are composed of  $\text{CaCO}_3$  with other mineral phases typically only present in the form of detrital material attached to the surface or incorporated into large cracks. The only exception was belemnite C2 (*jason* subzone) where pyrite had infiltrated a small portion of a growth ring (less than 300 $\mu\text{m}$  long) immediately adjacent to a large ventral crack, again an area easily avoided in sampling.

Despite the less promising CL findings for specimens from the *medea* subzone it was decided to proceed with the sampling of one specimen of *G. (B.) dilobotes* and one specimen of *C.*

*puzosiana* from this subzone. The encouraging carbonate staining results, as well as the BSEM examinations suggested that the original crystal structures of these specimens had not been compromised.

For photomicrographs of the results of testing by CL, carbonate staining and electron microscopy, the reader is referred to supplementary material in the on-line version of this article.

**Fig.6. Through ontogeny  $\delta^{18}\text{O}$  and  $\delta^{13}\text{C}$  for *G. (B.) dilobotes* and *C. puzosiana***

**Table 1. Isotope data for specimens of *G. (B.) dilobotes***

**Table 2. Isotope data for specimens of *C. puzosiana***

#### 4.2. Isotope data

##### 4.2.1. *Gryphaea* – G1

Incremental  $\delta^{18}\text{O}$  values for G1 (Fig. 6A) vary from  $-1.20\text{‰}$  ( $16.9^\circ\text{C}$ ) to  $-0.47\text{‰}$  ( $13.8^\circ\text{C}$ ), with an arithmetic mean value of  $-0.71\text{‰}$  ( $14.8^\circ\text{C}$ ) and a range of  $0.73\text{‰}$  ( $3.0^\circ\text{C}$ ). There is a cyclical pattern to the data with relative depletion of  $^{18}\text{O}$  recorded at two points: at shell height 5mm, where  $\delta^{18}\text{O}$  is  $-0.96\text{‰}$  ( $15.8^\circ\text{C}$ ), and in later ontogeny at shell height 22mm, where  $\delta^{18}\text{O}$  falls to  $-1.20\text{‰}$  ( $16.9^\circ\text{C}$ ).

Incremental  $\delta^{13}\text{C}$  data (Fig. 6A) vary from  $2.04\text{‰}$  to  $2.88\text{‰}$ , with an arithmetic mean value of  $2.53\text{‰}$  and a range of  $0.84\text{‰}$ . These data fall within a range from  $2.35\text{‰}$  to  $2.88\text{‰}$  throughout ontogeny, with two exceptions. Between shell heights 2mm and 5mm  $^{13}\text{C}$  is somewhat

depleted and  $\delta^{13}\text{C}$  falls to 2.05‰. Further relative depletion of  $^{13}\text{C}$  is recorded at shell height 24mm where  $\delta^{13}\text{C}$  falls to a minimum for this specimen of 2.04‰.

#### *Anomalous and missing data for G. (B.) dilobotes specimen G1*

Gaps are visible in the data sets displayed in Fig. 6 for specimen G1. The data gap at shell height 23mm was due to anomalous values of  $-6.20\text{‰}$  for  $\delta^{18}\text{O}$  and  $0.80\text{‰}$  for  $\delta^{13}\text{C}$  at this point. At shell height 28mm there is a second gap composed of two sample points. The first of these returned results of  $-4.54\text{‰}$  for  $\delta^{18}\text{O}$  and  $1.20\text{‰}$  for  $\delta^{13}\text{C}$ . These two anomalous results were fully expected as cracks in the shell were noted at these sample points. However, these points were still sampled in ontogenetic sequence in order to assess the effects of sampling obviously altered material. The second gap at 28mm reflects nil return of data. The anomalous data are included in Table 1.

#### *4.2.2. Gryphaea – G2*

Incremental  $\delta^{18}\text{O}$  values for G2 (Fig. 6B) vary from  $-1.14\text{‰}$  ( $16.6^\circ\text{C}$ ) to  $-0.55\text{‰}$  ( $14.2^\circ\text{C}$ ), with an arithmetic mean value of  $-0.82\text{‰}$  ( $15.3^\circ\text{C}$ ) and a range of  $0.59\text{‰}$  ( $2.4^\circ\text{C}$ ). There is a relative depletion of  $^{18}\text{O}$  from the umbo up to shell height 10mm, with a minimum  $\delta^{18}\text{O}$  value in this section of shell of  $-1.14\text{‰}$  ( $16.6^\circ\text{C}$ ) at the first sample point. From shell height 10mm  $\delta^{18}\text{O}$  values record a relative enrichment of  $^{18}\text{O}$ . The maximum  $\delta^{18}\text{O}$  value in this section of shell is  $-0.55\text{‰}$  ( $14.2^\circ\text{C}$ ), recorded twice between shell heights of 15 and 20mm.

Incremental  $\delta^{13}\text{C}$  data (Fig. 6B) vary from  $2.01\text{‰}$  to  $3.08\text{‰}$ , with an arithmetic mean value of  $2.59\text{‰}$  and a range of  $1.07\text{‰}$ . There is a relative depletion of  $^{13}\text{C}$  in early ontogeny, where  $\delta^{13}\text{C}$  falls to  $2.01\text{‰}$  at a shell height of 5mm. From shell height 9mm there is a relative

enrichment in  $^{13}\text{C}$  up to 3.08‰ at 17mm. The  $\delta^{13}\text{C}$  values are then lower until shell height 20mm and then remain relatively stable at around 2.50‰ throughout the remaining sampled ontogeny, albeit with a spike to c. 3‰ at the last sample point.

#### 4.2.3. *Gryphaea* - G3

Incremental  $\delta^{18}\text{O}$  values for G3 (Fig. 6C) vary from  $-1.24\text{‰}$  ( $17.0^\circ\text{C}$ ) to  $-0.44\text{‰}$  ( $13.7^\circ\text{C}$ ), with an arithmetic mean value of  $-0.61\text{‰}$  ( $14.4^\circ\text{C}$ ) and a range of  $0.80\text{‰}$  ( $3.3^\circ\text{C}$ ). There is a depletion of  $^{18}\text{O}$  up to shell height of 10mm, where there is a  $\delta^{18}\text{O}$  minimum value of  $-1.24\text{‰}$  ( $17.0^\circ\text{C}$ ). The maximum  $\delta^{18}\text{O}$  value of  $-0.44\text{‰}$  ( $13.7^\circ\text{C}$ ) is recorded at shell height 29mm.

Incremental  $\delta^{13}\text{C}$  data (Fig. 6C) vary from  $2.23\text{‰}$  to  $3.01\text{‰}$ , with an arithmetic mean value of  $2.65\text{‰}$  and a range of  $0.78\text{‰}$ . There is a relative depletion of  $^{13}\text{C}$  in early ontogeny, with  $\delta^{13}\text{C}$  of  $2.23\text{‰}$  recorded at shell height 10mm. Beyond 10mm  $\delta^{13}\text{C}$  values record relative enrichment in  $^{13}\text{C}$ , up to  $2.99\text{‰}$  at a shell height of 11mm and  $3.01\text{‰}$  at 22mm. From 22mm there is a trend towards relative depletion in  $^{13}\text{C}$ , although not to the low levels seen in the umbo and notwithstanding an isolated high value of  $2.85\text{‰}$  for  $\delta^{13}\text{C}$  at 44mm.

#### 4.2.4. *C. puzosiana* – C1

Incremental  $\delta^{18}\text{O}$  values for C1 (Fig. 6D) vary from  $-0.59\text{‰}$  ( $14.3^\circ\text{C}$ ) to  $0.18\text{‰}$  ( $11.3^\circ\text{C}$ ), with an arithmetic mean value of  $-0.11\text{‰}$  ( $12.4^\circ\text{C}$ ), a range of  $0.77\text{‰}$  ( $3.1^\circ\text{C}$ ) and a broadly cyclical pattern. Relative depletion of  $^{18}\text{O}$  occurs up to 3mm from the apical canal, with  $\delta^{18}\text{O}$  to  $-0.39\text{‰}$  ( $13.5^\circ\text{C}$ ), and also occurs between 12mm from the apical canal and the rostrum edge where  $\delta^{18}\text{O}$  values fall to  $-0.59\text{‰}$  ( $14.3^\circ\text{C}$ ). Between 3 and 12mm from the apical canal

there is a relative enrichment in  $^{18}\text{O}$ , with the maximum  $\delta^{18}\text{O}$  value for this specimen of 0.18‰ (11.3°C) recorded in this section of rostrum.

Incremental  $\delta^{13}\text{C}$  data (Fig. 6D) vary from 1.04‰ to 3.37‰, with an arithmetic mean value of 2.10‰ and a range of 2.33‰. The maximum  $\delta^{13}\text{C}$  value for this specimen of 3.37‰ is recorded less than 1mm from the apical canal, whilst the minimum value of 1.04‰ is recorded adjacent to the rostrum edge. This reflects a trend of declining  $\delta^{13}\text{C}$  values through ontogeny, despite significant volatility in the  $\delta^{13}\text{C}$  data throughout the rostrum.

#### 4.2.5. *C. puzosiana* – C2

Incremental  $\delta^{18}\text{O}$  values for C2 (Fig. 6E) vary from  $-1.09$ ‰ (16.4°C) to 0.12‰ (11.5°C), with an arithmetic mean value of  $-0.35$ ‰ (13.4°C) and a range of 1.21‰ (4.8°C). There is a relative enrichment in  $^{18}\text{O}$  from the apical canal to 9mm from the apical canal, with the maximum  $\delta^{18}\text{O}$  value in this section of rostrum being 0.12‰ (11.5°C). There is a relative depletion in  $^{18}\text{O}$  from 9mm, with a minimum  $\delta^{18}\text{O}$  value for the specimen of  $-1.09$ ‰ (16.7°C) at 10.5mm from the apical canal. From this point there is an increasing enrichment in  $^{18}\text{O}$  as the rostrum edge is approached.

Incremental  $\delta^{13}\text{C}$  data (Fig. 6E) vary from 1.21‰ to 3.84‰, with an arithmetic mean value of 2.63‰ and a range also of 2.63‰. No overall trend is visible in these data but cyclic variations in  $\delta^{13}\text{C}$  values are seen throughout ontogeny with only a minimal enrichment in  $^{13}\text{C}$  towards the outer edge of the rostrum.

#### 4.2.6. *C. puzosiana* – C3

Incremental  $\delta^{18}\text{O}$  values for C3 (Fig. 6F) vary from  $-1.04\text{‰}$  ( $16.2^\circ\text{C}$ ) to  $0.32\text{‰}$  ( $10.8^\circ\text{C}$ ), with an arithmetic mean value of  $-0.45\text{‰}$  ( $13.8^\circ\text{C}$ ) and a range of  $1.36\text{‰}$  ( $5.4^\circ\text{C}$ ). There is a relative depletion in  $^{18}\text{O}$  between 5mm and 8mm from the apical canal, where the minimum  $\delta^{18}\text{O}$  value for this specimen of  $-1.04\text{‰}$  ( $16.2^\circ\text{C}$ ) is recorded. From 8mm from the apical canal a trend towards enrichment in  $^{18}\text{O}$  is recorded, with a maximum  $\delta^{18}\text{O}$  value of  $0.32\text{‰}$  ( $10.8^\circ\text{C}$ ) at 11mm from the apical canal. From this sample point there is a progressive depletion in  $^{18}\text{O}$  as the rostrum edge is approached, with a  $\delta^{18}\text{O}$  value of  $-0.63\text{‰}$  ( $14.5^\circ\text{C}$ ) at 12mm from the apical canal. Areas close to the apical canal were not sampled.

Incremental  $\delta^{13}\text{C}$  data (Fig. 6F) vary from  $0.92\text{‰}$  to  $2.61\text{‰}$ , with an arithmetic mean value of  $2.14\text{‰}$  and a range of  $1.69\text{‰}$ . Missing data from early ontogeny for this specimen may obscure trends which would be apparent with a fuller data set, and as with other belemnites sampled these  $\delta^{13}\text{C}$  data show significant variability making meaningful trends difficult to identify.

#### 4.3. Comparing *jason* and *medea* subzones.

Stable isotope data from specimens G1, G2, C1, C2 (*Kosmoceras (Gulielmiceras) jason* ammonite subzone) and G3, C3 (*Kosmoceras (Gulielmiceras) medea* subzone) reveal no significant difference in environmental conditions between horizons. The arithmetic mean  $\delta^{18}\text{O}$  from G3 (*medea*) of  $-0.61\text{‰}$  ( $14.4^\circ\text{C}$ ) is higher than the values of  $-0.71\text{‰}$  ( $14.8^\circ\text{C}$ ) and  $-0.82\text{‰}$  ( $15.3^\circ\text{C}$ ) for G1 and G2 (*jason*), but G3 has the largest range at  $0.80\text{‰}$  ( $3.3^\circ\text{C}$ ) compared to  $0.73\text{‰}$  ( $3.0^\circ\text{C}$ ) and  $0.59\text{‰}$  ( $2.4^\circ\text{C}$ ) for G1 and G2. The  $\delta^{13}\text{C}$  values from *Gryphaea* from different horizons also broadly correspond, with an arithmetic mean of  $2.53\text{‰}$

for G1; 2.59‰ for G2 (*jason*); and 2.65‰ for G3 (*medea*). The ranges for these specimens are 0.84‰ for G1; 1.07‰ for G2 (*jason*); and 0.78‰ for G3 (*medea*).

The arithmetic mean  $\delta^{18}\text{O}$  values from *Cylindroteuthis* are also similar across subzones although C1 (*jason*) has the highest value at  $-0.11\text{‰}$  ( $12.4^{\circ}\text{C}$ ) compared to values of  $-0.35\text{‰}$  ( $13.4^{\circ}\text{C}$ ) for C2 (*jason*) and  $-0.45\text{‰}$  ( $13.8^{\circ}\text{C}$ ) for C3 (*medea*). Specimen C3 has the largest intra-rostrum range at  $1.36\text{‰}$  ( $5.4^{\circ}\text{C}$ ), whilst specimens from the *jason* subzone display smaller ranges of  $0.77\text{‰}$  ( $3.1^{\circ}\text{C}$ ) for C1 and  $1.21\text{‰}$  ( $4.8^{\circ}\text{C}$ ) for C2. Belemnite rostra provide arithmetic mean  $\delta^{13}\text{C}$  values of  $2.10\text{‰}$  for specimen C1;  $2.63\text{‰}$  for C2 (*jason*); and  $2.14\text{‰}$  for C3 (*medea*). The ranges for these specimens are  $2.33\text{‰}$  for C1;  $2.63\text{‰}$  for C2 (*jason*); and  $1.69\text{‰}$  for C3 (*medea*).

## 5. Discussion

### 5.1. General findings

The stable isotope data presented in 4.1 to 4.3 point to a Callovian environment which remained stable across the transition from the *jason* to *medea* subzone. *G. (B.) dilobotes* specimens record annual mean benthic temperatures of c.  $15^{\circ}\text{C}$  with ranges of c.  $3^{\circ}\text{C}$ , whilst *C. puzosiana* specimens record mean temperatures of c.  $13^{\circ}\text{C}$  with ranges between c.  $3^{\circ}\text{C}$  and c.  $5.5^{\circ}\text{C}$ . Both taxa record  $\delta^{13}\text{C}$  values of c.  $2\text{‰}$  to c.  $3\text{‰}$ , although *C. puzosiana* records ranges in excess of  $2\text{‰}$ , whilst *G. (B.) dilobotes* records ranges of c.  $1\text{‰}$ . The slightly less promising preservation of specimens from the *medea* subzone in comparison to the *jason* subzone (section 4.1) appears to have had no impact upon isotope data as results are consistent between horizons (see 4.3).

## 5.2. $\delta^{18}\text{O}$ palaeotemperatures

### 5.2.1. *Gryphaea (Bilobissa) dilobotes*

Arithmetic mean palaeotemperatures from *G. (B.) dilobotes* of around 15°C fall towards the lower end of the range of previously published estimates of average benthic palaeotemperatures from the Peterborough Member. These published  $\delta^{18}\text{O}$  data from *Ostrea*, *Mesosaccella* and *Nuculoma* indicate temperatures of c.14 to 16°C when they are re-adjusted for  $\delta^{18}\text{O}_{\text{seawater}}$  at -1‰ (Hudson, 1978), whilst data from *Gryphaea* sp. suggest average benthic temperatures of c. 17°C (Anderson et al., 1994). Unfortunately, these previous estimates are not based upon seasonally resolved data.

These mean palaeotemperatures from *G. (B.) dilobotes* are cooler than expected for a palaeolatitude of 35°N in the Jurassic. This expectation is based upon the widely accepted view that the Jurassic was a greenhouse world (Frakes et al., 1992; Sellwood and Valdes, 1997; Poulsen and Riding, 2003; Brigaud et al., 2008) and hence at this time sites at comparable latitudes should have experienced comparable or warmer temperatures than similar latitudes under modern conditions. Anderson et al. (1994) and Hudson (1978) suggest mean SSTs for this time of c. 20°C, which broadly correspond with those of similar latitudes today (Johnson et al., 2009). We propose that the most likely explanation for these cool palaeotemperatures from *G. (B.) dilobotes* is depth of habitat, an interpretation supported by the fine sediments from which the specimens were collected, sediments which would have required unagitated conditions for deposition. Under such circumstances, thermal stratification may develop during the summer, with the result that conditions at the seafloor are substantially cooler than those at the surface during this season, leading to muted seasonal variation and cooler annual mean benthic temperatures.

An approximate depth can be suggested for these *Gryphaea* if reference is made to the modern Gulf of Tunis, where SSTs range from 14°C in winter to 26°C in summer (Johnson et al., 2009) and where the median of these temperatures is comparable with average English Callovian SSTs of c. 20°C as established by Hudson (1978) and Anderson et al. (1994). Despite a surface seasonal range of 12°C at the Gulf of Tunis, seasonality at depth is restricted, and at 50m temperatures only fluctuate between c.15°C and c.17°C (Johnson et al., 2009), which is broadly comparable with the range identified in *G. (B.) dilobotes* here (from 14°C or less up to c. 17°C). This suggests a habitat at similar depth and broadly concurs with previously published maximum depth estimates for these waters of 30 – 50m (Hudson and Martill, 1991).

Cool temperatures from *G. (B.) dilobotes* might also be related to the influence of oceanic currents. Dera et al. (2009) suggest that currents may have flowed southwards between the islands of the northern European sea during the early part of the Jurassic, based upon neodymium isotope evidence. Southward flowing currents are likewise invoked by Lécuyer et al. (2003) to explain unexpectedly high  $\delta^{18}\text{O}$  values from the Bathonian onwards recorded by fossils in the Paris Basin.

Another potential modern analogue, which is more open than the Mediterranean and also subject to cool currents from the north, is the Sea of Japan. In the most southerly part of this channel, off the coast near Hiroshima (at 35° north and 135° east), mean annual SSTs are c. 19°C (JODC, undated), slightly cooler than comparable latitudes in the Mediterranean and the English Callovian. Annual minimum temperatures at 50m depth in the southern Sea of Japan

are  $10.9^{\circ}\text{C} \pm 0.2^{\circ}\text{C}$ , recorded in March, and maxima are  $22.0^{\circ}\text{C} \pm 0.6^{\circ}\text{C}$ , in September (JODC, undated). This gives a much higher range of c.  $11^{\circ}\text{C}$  than the range of c.  $3^{\circ}\text{C}$  recorded by our Callovian *Gryphaea*. An almost identical range to that recorded by *G. (B.) dilobotes* could only be possible at 50m depth in the extremely unlikely scenario where the maximum recorded March value (c.  $13^{\circ}\text{C}$ ) and the minimum September value (c.  $16^{\circ}\text{C}$ ) occur in the same calendar year.

The above comparisons lead us to conclude that a habitat at c. 50m, within or below a seasonal thermocline, is the most likely explanation for cool benthic palaeotemperatures and restricted seasonality shown by the isotopic evidence from specimens of *G. (B.) dilobotes*. The presence of strong, cool southward flowing currents in the Callovian seems unlikely as the narrow potential conduits to the north would have restricted such flows (see for example Bradshaw et al., 1992 for palaeogeographical information). Further, and importantly, the waters in which the Peterborough Member was deposited were anoxic for the vast majority of the time (Kenig et al., 2004). Such low oxygen conditions are unlikely in the presence of strong oceanic currents.

Data from early ontogeny of all three specimens of *G. (B.) dilobotes* suggests that shell growth in the first year began and continued throughout the summer, although some variation exists in the expression of temperature changes in later ontogeny. Specimen G1 shows a warm temperature peak in the juvenile life stage and a second period of high temperatures at shell height 22mm (fig. 6). Obvious seasonality is lacking in the later ontogeny of specimens G2 and G3. These patterns may suggest that specimens G2 and G3 experienced rapid early growth, and that data extracted represent less than a full year. It is of note that such a strong

signal of rapid summer growth may be unique to early life, as previous authors have argued for a summer growth hiatus in *Gryphaea* (Jones and Gould, 1999). Alternatively it may be that the length of this first summer was exaggerated by the method of sampling. In the early stages of ontogeny sampling was at a shallower angle to growth increments, whilst in later growth stages the line of sampling was at a higher angle to growth increments.

### 5.2.2. *Cylindroteuthis puzosiana*

Arithmetic mean palaeotemperatures from *C. puzosiana* are c. 13°C. These average values are broadly comparable with temperatures from other Callovian belemnites (e.g. Nunn et al., 2009; Wierzbowski et al., 2009; Anderson et al., 1994, Li and McArthur, 2013). Intra-rostrum temperature ranges of c. 3°C to c. 5.4°C in this study are also similar to those reported in previous studies for other belemnite species. These studies suggest ranges of c. 2°C from Bathonian (Jurassic) belemnites (Wierzbowski and Joachimski, 2009); c. 6.5°C from Toarcian (Jurassic) belemnites (McArthur et al., 2007); c. 3°C from Early Cretaceous belemnites (Price et al., 2012); c. 5°C from Late Cretaceous belemnites (Dutton et al., 2007) and a range of c. 4°C from a single specimen of *C. puzosiana*, from the *jason* zone of the Peterborough Member (Kings Dyke, Whittlesey) (Li and McArthur, 2013).

Mean  $\delta^{18}\text{O}$  palaeotemperatures from *C. puzosiana* are cooler than the average palaeotemperature from any specimen of *G. (B.) dilobotes*, with the warmest belemnite mean temperature being 13.8°C (C3), compared to the coolest *Gryphaea* mean temperature of 14.4°C (G3). Some temperatures derived from portions of earlier ontogeny in *C. puzosiana* are, however, significantly cooler than the minimum recorded for this locality by *G. (B.) dilobotes*, falling as low as 11.3°C (C1) 11.5°C (C2) and 10.7°C (C3). These cool

temperatures are interpreted here as being a consequence of migration, a possible behavioural characteristic of some belemnite species (e.g. Doyle and Macdonald, 1993; McArthur et al., 2007; Price and Page, 2008; Alberti et al., 2012; Li et al., 2012).

The highest  $\delta^{18}\text{O}$  values from the rostra of *C. puzosiana* could reflect a portion of life spent in cooler waters a significant distance to the north of the site of collection. In order to estimate an absolute maximum range for this proposed migration it is useful to draw comparisons with modern sea temperatures. As stated previously (section 5.2.1) similar benthic conditions to those recorded by *G. (B.) dilobotes* are seen in the modern Gulf of Tunis at depths of approximately 50 m, and the temperature range here also matches  $\delta^{18}\text{O}$  palaeotemperatures from some portions of life from *C. puzosiana*. However, were *C. puzosiana* to be alive today, then in order to experience temperatures as low as 11°C at a depth of 50 m individuals would have to migrate from the Mediterranean to waters near Brittany, France (for 11°C in winter) or northern Scotland, UK (11°C in summer) (NOAA, 2009), a change in latitude from 37°N to approximately 48°N and 58°N, respectively. Whilst differences in palaeogeography and ocean currents prevent such data being directly applied to the Jurassic, this comparison nevertheless strongly suggest that considerable distances were travelled.

Depth of habitat has been invoked to explain a combination of cool temperatures and muted intra-rostrum isotope palaeotemperature ranges in studies where an incremental approach to the determination of  $\delta^{18}\text{O}$  was employed (e.g. Dutton et al., 2007; Wierzbowski and Joachimski, 2009; Price et al., 2012), and in studies where average belemnite  $\delta^{18}\text{O}$  palaeotemperatures were lower than those derived from proxies believed to represent SSTs, e.g.  $\text{TEX}_{86}$  (Mutterlose et al., 2010; 2012),  $\delta^{18}\text{O}$  from pelagic fish teeth (Dera et al., 2009), and

$\delta^{18}\text{O}$  from whole rock carbonate, composed of nanoplankton and transported platform ooze (Boden et al., 2009).

In the present case, depth of belemnite habitat alone cannot explain the significant offset in the temperature minima between belemnites and benthos revealed here by incremental analyses. In order to record minimum temperatures of  $11^\circ\text{C}$  without migrating laterally, *C. puzosiana* would have had to dive to considerable depths. In modern settings where SST averages around  $20^\circ\text{C}$ , as suggested for English Callovian waters (Hudson, 1978; Anderson et al., 1994), it would be necessary to descend to approximately 1000m to reach waters at  $11^\circ\text{C}$  (Pierre, 1999). Such activities for *C. puzosiana* are unlikely for two reasons. Firstly, because analyses of the morphology of the thin aragonite septa of belemnite phragmocones suggest that the maximum hydrostatic pressure that they could tolerate would have restricted them to shelf seas (Arkhipkin et al., 2012; Wierzbowski, 2004). In particular, work by Westermann (1973), which suggests that *Cylindroteuthis* may have had unusually high water pressure tolerances for a belemnite, still shows that it could not have reached depths of 1000m, having a theoretical maximum tolerance of 600m and probably never exceeding 400m. Secondly, the palaeogeography and palaeobathymetry established by Bradshaw et al. (1992) for North West Europe in the Callovian argues against depths of 1000m, whilst Hudson and Martill (1991) established that during the time of deposition of the Peterborough Member there were no waters deeper than 50m within 150km of the Midlands Platform.

It is possible that moderate depth could contribute to these cool belemnite palaeotemperatures. However, access to appropriate depths in the Callovian of Europe, would still have required a migration of c. 500 miles or 800km (or c.  $5^\circ$  of latitude), as the

nearest deep waters were probably in the Faeroe and Rockall rift zones, to the west of modern Scotland (Bradshaw et al., 1991; Ziegler, 1990). Based upon modern latitudinal gradients (NOAA, 2009), mean SSTs in these Jurassic rifts were probably c. 18°C, around c. 2°C cooler than waters in central England. In modern contexts where similar mean SSTs are observed, e.g. off the coast of Portugal, temperatures at c. 300m never vary outside a range of 10-11°C. This suggests that in these northerly rift zones *C. puzosiana* could record cool  $\delta^{18}\text{O}$  palaeotemperatures with a less extensive migration than into Boreal waters.

Thierry et al. (2000) also suggest that deep waters may have been present in the Tethyan realm in the Jurassic, corresponding to areas in modern central and southern Europe, but if *C. puzosiana* were recording cool temperatures due to deep water habitats at these southerly palaeolatitudes this still implies significant migration. These deep Tethyan waters may, however, account for some cool belemnite palaeotemperatures, for example those reported in Submediterranean/Mediterranean belemnites in comparison to Subboreal/Boreal belemnites in the Oxfordian-Early Kimmeridgian of the Jurassic (e.g. Wierzbowski, 2004). In this study  $\delta^{18}\text{O}$  temperatures from Subboreal/Boreal *Cylindroteuthis* sp. and *Pachyteuthis* sp. (Isle of Skye, Scotland) were comparable or warmer than the  $\delta^{18}\text{O}$  temperatures from Mediterranean/Tethyan *Hibolithes* sp. and *Belemnopsis* sp. These Tethyan belemnites are unlikely to have migrated into and out of cool Boreal waters, being absent from the fossil record in this region (Doyle, 1987) and so vertical rather than lateral migration, an option not open to *C. puzosiana* due to bathymetric constraints in English waters, may be an explanation. It must be noted however that Wierzbowski (2004) reports that a maximum depth for these more southerly genera is only some 150–200m. Clearly this is an area for further consideration, but unfortunately, whilst interesting, is beyond the remit of this study.

Incremental  $\delta^{18}\text{O}$  signals displayed in Fig.6 give end-ontogeny temperatures experienced by *C. puzosiana* of 14.3°C (C1) 13.6°C (C2) and 14.5°C (C3), which are close to winter temperatures determined for this locality from specimens of *G. (B.) dilobotes*. When one considers both the site of collection of these belemnites, along with the end-ontogeny isotope palaeotemperature data that these belemnites yield, this suggests that these belemnites were recording conditions in the same locale as *G. (B.) dilobotes*, around the time of their death. They may not have been living at the same depth, but life in a winter water column, where a thermocline has degraded, would return similar local  $\delta^{18}\text{O}$  data from both taxa, whatever their position above the sea bed. This issue requires further investigation as the rate of growth of belemnites in late ontogeny is unclear and growth may vary through life according to conditions and age, as seen in modern *Sepia* sp. (Hewitt and Stait, 1988). If belemnite growth slowed a significant time before death, then the  $\delta^{18}\text{O}$  signals from the rostrum edge of these *C. puzosiana* could represent cool  $\delta^{18}\text{O}$  palaeotemperatures from other localities, for different seasons, but any such speculation would be reliant upon the assumption that these specimens had reached the critical growth stage. However, given collection in the same locality for specimens of all taxa, and close correspondence between late-ontogeny  $\delta^{18}\text{O}$  values for all three belemnites and  $\delta^{18}\text{O}$  maxima for all *Gryphaea* specimens, it appears that these belemnites probably did precipitate calcite throughout life and died recording conditions close to the Whittlesey locale. Significantly, both scenarios suggest that migration over significant distances occurred. Such movements are plausible when one considers that the modern squid *Illex argentinus* traverses large latitudinal ranges in the shelf seas off South America (Arkhipkin, 2012), whilst *Sepia* sp. are also reported to migrate (Rexfort and Mutterlose, 2006).

Some recent papers have explained unexpectedly cool belemnite palaeotemperatures as being the result of salinity effects (Mutterlose et al., 2010; 2012). Scheurle and Hebbeln (2003) state that a  $\pm 1$  PSU change in salinity alters  $\delta^{18}\text{O}_{\text{carbonate}}$  by approximately  $\pm 0.35\text{‰}$  ( $1.4^\circ\text{C}$ ), although others such as Price and Sellwood (1997) suggest a smaller effect of  $\pm 0.25\text{‰}$  upon  $\delta^{18}\text{O}$ . This implies that a positive shift of  $0.8\text{‰}$  in  $\delta^{18}\text{O}$  (c.  $4^\circ\text{C}$ ), enough to account for the temperature disparity here, would require an increase in salinity of c. 2-3 PSU. However, such an explanation is unlikely to account for the cool belemnite temperatures recorded here. If it is assumed that *C. puzosiana* lived continuously in the same locality as *G. (B.) dilobotes*, then these belemnites can only have lived at or above the level occupied by *G. (B.) dilobotes* in the water column. As the salinity of water increases, so does its density, causing it to sink. Thus, benthic organisms should also be influenced by high salinity water, leading to higher benthic  $\delta^{18}\text{O}$  values as well. If cool temperatures from *C. puzosiana* are a reflection of highly saline conditions, they must have been encountered somewhere other than the study site.

Another explanation for an offset between average temperatures from belemnites and from *G. (B.) dilobotes* is that benthic organisms may be influenced through life by chemical interactions at the sediment-water interface. These are caused by the alteration of volcanoclastic material to clay, which may lead to anomalously low  $\delta^{18}\text{O}$  values (Price and Sellwood, 1997; Rosales et al., 2001; Price et al., 2012). Such processes are unlikely to have a strong effect in the present case, however, as the clay-rich sediments of the Peterborough Member are believed to have been recycled several times over a period of over 1Ga (Norry et al., 1994).

This final explanation for the unexpected difference between temperatures from *C. puzosiana* and from *G. (B.) dilobotes* is also undermined when one considers average  $\delta^{18}\text{O}$  data for all taxa sampled from the Peterborough Member in previously published studies. These data from ammonites and bivalves preserve normal vertical temperature gradients (Hudson, 1978; Anderson et al., 1994). This implies that the inverted temperature relationship between *G. (B.) dilobotes* and *C. puzosiana* is not due to *G. (B.) dilobotes* being unusually “warm” due to chemical effects at the sea bed. The lack of unexpectedly cool temperatures from SST indicators such as ammonites in these data suggests that the primary influence on cool temperatures in *C. puzosiana* was conditions experienced at a higher palaeolatitudes, or a combination of higher latitudes and deep water.

### 5.3. $\delta^{13}\text{C}$ and palaeoenvironmental conditions

#### 5.3.1. *Gryphaea (Bilobissa) dilobotes*

Arithmetic mean  $\delta^{13}\text{C}$  values of 2.53‰ for G1 and 2.59‰ for G2 (both *jason* subzone) and 2.65‰ for G3 (*medea* subzone) are comparable with other  $\delta^{13}\text{C}$  data for the English Callovian from *Gryphaea* sp. (Anderson et al., 1994). These data are also comparable with Jurassic belemnite data from England, Scotland and continental Europe (e.g., Anderson et al., 1994; Nunn et al., 2009; Wierzbowski et al., 2009; Wierzbowski and Joachimski, 2009; Nunn and Price, 2010), and also with modern ocean values (Rexfort and Mutterlose, 2006). Mean  $\delta^{13}\text{C}$  values of this magnitude are indicative of high rates of productivity, and/or enhanced preservation of biological matter at the seabed due to low levels of oxygenation (Nunn and

Price 2010), conditions which have been previously proposed for English Callovian waters (Bradshaw et al., 1992; Belin et al., 1994).

Sea floor anoxia in the Callovian may have been intermittent (Kenig et al., 2004), as suggested by the visible alternation between shell beds and organic-rich clay beds in the lower part of the Peterborough Member (e.g., the transitions between beds 9 to 11). The organic rich beds (e.g., bed 10) would have been deposited in periods of low oxygenation, but the shell beds would have been associated with levels of oxygen sufficiently high to support bivalves. These latter conditions may have reduced the preservation and burial of organics. Specimens for this study are all from shell beds (9 and 11) and thus representative of periods when oxygen levels would have been higher, indicating that  $\delta^{13}\text{C}$  data here are probably indicative of relatively high productivity.

Intra-shell analysis of  $\delta^{13}\text{C}$  for *G. (B.) dilobotes* shows that deviations from a relatively stable rate of fractionation are only significant in the juvenile stage of life where there is a depletion of  $^{13}\text{C}$  in all three specimens. These signals correspond with warm isotope palaeotemperatures but  $\delta^{13}\text{C}$  is only in-phase with isotope temperatures in this portion of the shell. These data perhaps suggest that low  $\delta^{13}\text{C}$  values represent the benthic oxidation of  $^{12}\text{C}$ -rich biomass, which may rain down upon the sea floor in later summer following plankton blooms. Similar explanations for such seasonal patterns showing  $^{12}\text{C}$  enriched (light)  $\delta^{13}\text{C}$  during warmer months and  $^{12}\text{C}$  depleted (heavy)  $\delta^{13}\text{C}$  in cooler months, for modern bivalves living at depths of c. 45m below a thermocline, have been proposed by Arthur et al. (1983). Beyond these early ontogenetic deviations, changes in  $\delta^{13}\text{C}$  are limited.

Whilst these data appear coherent, and the mean values are similar to those from other Callovian *Gryphaea* (Anderson et al., 1994), the problematic nature of interpreting  $\delta^{13}\text{C}$  data must be raised, as bivalve shell carbonate may be rendered isotopically light due to the incorporation of metabolically derived carbon, and intra-shell cycles in  $\delta^{13}\text{C}$  could be influenced by vital effects related to age or by changes in environment over time (Schöne et al., 2011; Steuber, 1999).

### 5.3.2. *Cylindroteuthis puzosiana*

As with data from *G. (B.) dilobotes*, the arithmetic mean  $\delta^{13}\text{C}$  values for *C. puzosiana* are broadly comparable with data for Jurassic belemnites from the UK and wider Europe (e.g., Anderson et al., 1994; Nunn et al., 2009; Nunn and Price, 2010; Wierzbowski et al., 2009; Wierzbowski and Joachimski, 2009) and also with modern ocean values (Rexfort and Mutterlose, 2006). Whilst calculated mean values from these specimens appear to broadly correspond with data from *G. (B.) dilobotes*, the intra-rostrum ranges are large (between c. 1.7 and c. 2.6‰) when compared to the maximum range from *G. (B.) dilobotes* of 1.07‰ (G2). One explanation for this is that these ranges and the high degree of through-ontogeny variability in comparison to *G. (B.) dilobotes*, may reflect an active migratory lifestyle.

If *C. puzosiana* were only recording environmental  $\delta^{13}\text{C}$  levels one would expect late ontogeny  $\delta^{13}\text{C}$  data from *C. puzosiana* to be broadly similar to winter  $\delta^{13}\text{C}$  values recorded by specimens of *G. (B.) dilobotes*, as is the case with  $\delta^{18}\text{O}$  values. However, in this locality, whilst specimens of *G. (B.) dilobotes* record  $\delta^{13}\text{C}$  values in a range from approximately c. 2.4‰ (for all three *Gryphaea*) up to a maximum of 3.08‰ (from specimen G2), only late ontogeny  $\delta^{13}\text{C}$  values from belemnite C3 (2.46‰) are similar to winter values for *G. (B.)*

*dilobotes*, whilst those from C1 (1.04‰) and C2 (3.84‰) fall significantly outside the local benthic winter range recorded by *G. (B.) dilobotes*. This is problematical if one considers belemnites to be accurate archives of palaeoenvironmental data, although it may be explained if we speculate that belemnites ceased accreting calcite a significant time prior to death and that the final stages of ontogeny are recording the ambient isotope signal of distant waters, where  $\delta^{13}\text{C}$  values differ, but where  $\delta^{18}\text{O}$  values are coincidentally similar. This scenario, however, seems unlikely given the discussion above regarding the correspondence between late ontogeny  $\delta^{18}\text{O}$  values of *C. puzosiana* and the winter  $\delta^{18}\text{O}$  values of *G. (B.) dilobotes*, along with the shared site of collection (see 5.2.2).

Through-ontogeny  $\delta^{13}\text{C}$  signals from *C. puzosiana* may be misleading due to the impact of a significant metabolic influence that may occur throughout life. Many authors argue that vital influences significantly overwrite environmental  $\delta^{13}\text{C}$  signals, thus complicating the analysis and interpretation of  $\delta^{13}\text{C}$  values from belemnites (e.g. Anderson et al., 1994; Price and Page, 2008; Žák et al., 2011). Further, high degrees of variability are noted in  $\delta^{13}\text{C}$  data from these specimens of *C. puzosiana* and similar significant fluctuations in intra-rostrum  $\delta^{13}\text{C}$  values from other belemnites have been previously ascribed to metabolic influences (Wierzbowski and Joachimski, 2009). Support for such proposals comes from a study of *Sepia officinalis*, which is commonly considered to be the best modern analogue for belemnites. In this study, Rexfort and Mutterlose (2006) found high levels of variability in incremental  $\delta^{13}\text{C}$  data from the cuttlebones of wild specimens, and, significantly, in the cuttlebones of specimens reared in conditions where isotopic conditions were controlled. This, they concluded, was strong evidence that modern coleoids exert a significant vital effect upon carbon isotope ratios in their calcified hard parts, and this may have also been the case for their ancient counterparts.

The disparity between the end ontogeny values from each of the belemnites in this study may therefore be due to vital effects which operate throughout life, and it is therefore perhaps unwise to attempt to draw palaeoenvironmental conclusions from belemnite  $\delta^{13}\text{C}$ .

## 6. Conclusions

Oxygen isotope values from *G. (B.) dilobotes* suggest that this species accurately recorded benthic palaeotemperatures of around 15°C, with a seasonal range of approximately 3°C. These data are consistent with a depth of around 50m, based upon comparison with data from a range of Callovian taxa in other studies, and from comparison with conditions in the modern Gulf of Tunis, this being considered the most suitable analogue. Further, this depth corresponds well with previously published estimates of seabed depth for this environment. Average  $\delta^{13}\text{C}$  signals support findings from other studies indicating that productivity in these seas was generally high, although the data here only represent periods when the seabed was sufficiently oxygenated to support bivalves. Correspondence between low  $\delta^{18}\text{O}$  and  $\delta^{13}\text{C}$  values revealed by sclerochronological analyses imply that benthic signals may have been controlled by a thermocline precluding mixing in summer and allowing a stratified carbon isotope signal to develop.

The mean  $\delta^{18}\text{O}$  values from *C. puzosiana* are significantly higher (cooler) than values from *G. (B.) dilobotes*, whilst intra-rostrum signals reveal significantly cooler temperatures than the minima from *G. (B.) dilobotes*. These data suggest the possibility of extensive geographical migration by *C. puzosiana*, to sites at higher latitudes and/or locations where there was access to deeper waters, as other explanations such as diving into local deep waters or the influence of local high salinity water bodies influencing  $\delta^{18}\text{O}$  derived palaeotemperatures in *C.*

*puzosiana* can be discounted. Whether these movements were due to reproductive requirements, the search for food, or the result of other influences is unknown and further investigation is required. Whilst average  $\delta^{13}\text{C}$  signals from this taxon are comparable to those from other Jurassic sources and modern values from productive settings, incremental isotopic data are difficult to reconcile with behavioral or environmental influences. *C. puzosiana* records significantly wider ranges of  $\delta^{13}\text{C}$  through ontogeny than *G. (B.) dilobotes*, and is also displays much more short-term variability. This could be due to this taxon pursuing the proposed migratory lifestyle, and recording a range of diverse environments, although this is not necessarily supported by late ontogeny data. The data lead to the conclusion that whilst *C. puzosiana* may provide a reasonable long-term representation of the carbon profile of the waters in which it lived, metabolic influences may introduce extensive short-term variation into the  $\delta^{13}\text{C}$  signals.

This study highlights the importance of adopting a sclerochronological approach to the acquisition of isotope data. Isotopic values may vary through ontogeny and so the extraction of random point samples alone, from bivalves for example, may give accurate data, but the season it represents will remain unknown, whilst in the case of belemnites the geographical locality represented by isotope values may be unclear. This conclusion has particular importance with regard to the practice of relying upon isotope signals extracted from ontogenetically different portions of rostra taken from various belemnites, which may be of different species, in order to examine palaeoenvironmental evolution over geological time. Data presented here suggest that in the case of *C. puzosiana*, only the very latest stages of ontogeny reflect temperatures at the site of collection, whilst signals representing dissolved inorganic carbon may be obscured by vital influences.

## Acknowledgements

The authors wish to thank the anonymous reviewers whose valuable comments have helped to improve this paper. We also thank Professor John D. Hudson and Dr Keith L. Duff for helpful comments at Must Farm Quarry; members of Stamford and District Geological Society and Hanson PLC for arranging and allowing access to sites; Matthew Hunt and other technical staff at the University of Derby, along with Michael Maus and the technical staff at the University of Mainz; Steve Hodson, Neil Green and Richard Hannaford in Academic Graphics, University of Derby.

## Supplementary material

Supplementary material associated with this article can be found in the online version.

## References

Alberti, M., Fürsich, F.T., Pandey, D.K., 2012. The Oxfordian stable isotope record ( $\delta^{18}\text{O}$ ,  $\delta^{13}\text{C}$ ) of belemnites, brachiopods, and oysters from the Kachchh Basin (western India) and its potential for palaeoecologic, palaeoclimatic, and palaeogeographic reconstructions.

*Palaeogeography, Palaeoclimatology, Palaeoecology* 344–345, 49–68.

Anderson, T.F., Arthur, M.A., 1983. Stable isotopes of oxygen and carbon and their application to sedimentologic and environmental problems, in: Arthur, M.A., Anderson, T.F., Kaplan, I.R., Veizer, J., Land, L. S. (Eds.), *Stable Isotopes in Sedimentary Geology: Society of Economic Paleontologists and Mineralogists, Short Course Notes 10*, pp.1-151.

Anderson, T.F., Popp, B.N., Williams, A.C., Ho, L.-Z., Hudson, J.D., 1994. The stable isotopic record of fossils from the Peterborough Member, Oxford Clay Formation (Jurassic), UK: palaeoenvironmental implications. *Journal of the Geological Society, London* 151, 125-138.

Arkhipkin, A.I., 2012. Squid as nutrient vectors linking Southwest Atlantic marine ecosystems. *Deep Sea Research Part II: Topical Studies in Oceanography*. 95, 7-20

Arkhipkin, A.I., Bizikov, V.A., Fuchs, D., 2012. Vestigial phragmocone in the gladius points to a deepwater origin of squid (Mollusca: Cephalopoda). *Deep Sea Research Part I: Oceanographic Research Papers* 61, 109-122.

Arthur, M.A., Williams, D.F., Jones, D.S., 1983, Seasonal temperature-salinity changes and thermocline development in the mid-Atlantic Bight as recorded by the isotopic composition of bivalves. *Geology* 11, 655-659.

Barbin, V., Ramseyer, K., Debemay, J.P., Schein, E., Roux, M., Decrouez, D., 1991. Cathodoluminescence of Recent biogenic carbonates: an environmental and ontogenetic fingerprint. *Geological Magazine* 128, 19-26.

Barbin, V., Brand, U., Hewitt, R. A., Ramseyer, K., 1994, Similarity in cephalopod shell biogeochemistry since Carboniferous: evidence from cathodoluminescence. *Geobios* 28, 701-710.

Belin, S., Kenig, F., 1994. Petrographic analyses of organo-mineral relationships: depositional conditions of the Oxford Clay Formation (Jurassic), UK. *Journal of the Geological Society, London* 151, 153-160.

Bodin, S., Fiet, N., Godet, A., Matera, V., Westermann, S., Clément, A., Janssen, N.M.M., Stille, P., Föllmi, K.B., 2009. Early Cretaceous (late Berriasian to early Aptian) palaeoceanographic change along the northwestern Tethyan margin (Vocontian Trough, southeastern France):  $\delta^{13}\text{C}$ ,  $\delta^{18}\text{O}$  and Sr-isotope belemnite and whole-rock records *Cretaceous Research* 30, 1247-1262.

Bradshaw, M.J., Cope, J.C.W., Cripps, D.W., Donovan, D.T., Howarth, M.K., Rawson, P.F., West, I.M., Wimbledon, W.A., 1992. Jurassic, in: Cope, J.C.W., Ingham, J.K., Rawson, P.F. (Eds.), *Atlas of Palaeogeography and Lithofacies*. Geological Society Memoir 13, pp 107-130.

Brigaud, B., Pucéat, E., Pellenard, P., Vincent, B., Joachimski, M.M., 2008. Climatic fluctuations and seasonality during the Late Jurassic (Oxfordian – Early Kimmeridgian)

inferred from  $\delta^{18}\text{O}$  of Paris Basin oyster shells. *Earth and Planetary Science Letters* 273, 58-67.

Dera, G., Pucéat, E., Pellenard, P., Neige, P., Delsate, D., Joachimski, M.M., Reisberg, L., Martinez, M., 2009. Water mass exchange and variations in seawater temperature in the NW Tethys during the Early Jurassic: Evidence from neodymium and oxygen isotopes of fish teeth and belemnites. *Earth and Planetary Science Letters* 286, 198-207.

Dickson, J.A.D., 1965. A Modified Staining Technique for Carbonates in Thin Section. *Nature* 4971, 587.

Doyle, P., Macdonald, D.I.M., 1993. Belemnite Battlefields. *Lethaia* 26, 65-80.

Doyle, P 1987. Lower Jurassic-Lower Cretaceous belemnite biogeography and the development of the Mesozoic Boreal Realm. *Palaeogeography. Palaeoclimatology. Palaeoecology* 61, 237-254.

Duff, K.L., 1978. *Bivalvia from the English Lower Oxford Clay (Middle Jurassic)*. Monograph of the Palaeontological Society, London.

Dunca, E., Doguzhaeva, L., Schöne, B.R., van de Schootbrugge, B., 2006. Growth patterns in rostra of the Middle Jurassic belemnite *Megateuthis giganteus*: Controlled by the moon? *Acta Universitatis Carolinae – Geologica* 49, 107-117.

Dutton, A., Huber, B.T., Lohman, K.C., Zinsmeister, W.J., 2007. High-resolution stable isotope profiles of a *Dimitobelid* belemnite: implications for paleodepth habitat and Late Maastrichtian climate seasonality. *Palaios* 22, 642-650.

Frakes, L.A., Francis, J E., Syktus, J. I., 1992. *Climate modes of the Phanerozoic*. Cambridge University Press, New York.

Heilmayer, O., Brey, T., Storch, D., Mackensen, A., Arntz, W.E., 2004. Population dynamics and metabolism of *Aequipecten opercularis* (L) from the western English Channel (Roscoff – France). *Journal of Sea Research* 52, 33-44.

Hewitt, R.A., Stait, B., 1988. Seasonal variation in septal spacing of *Sepia officinalis* and some Ordovician actinocerid nautiloids. *Lethaia* 21, 383–394.

Hudson, J.D., 1978. Concretions, isotopes, and the diagenetic history of the Oxford Clay (Jurassic) of central England. *Sedimentology* 25, 339-370.

Hudson, J.D., Martill, D.M., Page, K.N. 1991. Introduction, in: Martill, D.M., Hudson, J.D. (Eds.), Fossils of the Oxford Clay. Palaeontological Association Field Guide to Fossils: 4, 11-34.

Hudson, J.D., Martill, D.M., 1991. The Lower Oxford Clay: production and preservation of organic matter in the Callovian (Jurassic) of central England. Geological Society, London, Special Publications. 58, 363-379.

Hudson, J.D., Martill, D.M., 1994. The Peterborough Member (Callovian, Middle Jurassic) of the Oxford Clay Formation at Peterborough, UK. Journal of the Geological Society, London 151, 113-124.

Johnson, A.L.A., Hickson, J.A., Bird, A., Schöne, B.R., Balson, P.S., Heaton, T.H.E., Williams, M., 2009. Comparative sclerochronology of modern and mid-Pliocene (c. 3.5 Ma) *Aequipecten opercularis* (Mollusca, Bivalvia): an insight into past and future climate change in the north-east Atlantic region. Palaeogeography, Palaeoclimatology, Palaeoecology 284, 164–179.

JODC, Undated. Oceanographic Data and Information download service (Temperature, Current, Depth, Biology, Marine information). Japan Oceanographic Data Centre. [Online]. Available at: <http://www.jodc.go.jp/index.html>

Jones, D.S., Gould, S.J., 1999. Direct measurement of age in fossil *Gryphaea*: the solution to a classic problem in heterochrony. *Paleobiology* 25, 158-187.

Kenig, F., Hayes, J.M., Popp, B.N., Summons, R. E., 1994. Isotopic biogeochemistry of the Oxford Clay Formation (Jurassic), UK. *Journal of the Geological Society, London* 151, 139-152.

Kenig, F., Hudson, J.D., Damsté, J.S.S. and Popp, B.N., 2004. Intermittent euxinia: Reconciliation of a Jurassic black shale with its biofacies. *Geology* 32, 412-424.

Lartaud, F., de Rafelis, M., Ropert, M., Emmanuel, L., Geairon, P., Renard, M., 2010. Mn labelling of living oysters: Artificial and natural cathodoluminescence analyses as a tool for age and growth rate determination of *C. Gigas* (Thunberg, 1793) shells. *Aquaculture* 300, 206-217.

Lécuyer, C., Picard, S., Garcia, J-P., Sheppard, S.M.F., Grandjean, P., Dromart, G., 2003. Thermal evolution of Tethian surface waters during the Middle-Late Jurassic: Evidence from  $\delta^{18}\text{O}$  values of Marine fish teeth. *Paleoceanography* 18, 1076.

Li, Q., McArthur, J.M., Atkinson, T.C., 2012. Lower Jurassic belemnites as indicators of palaeo-temperature. *Palaeogeography, Palaeoclimatology, Palaeoecology* 315–316, 38-45.

Li, Q., McArthur, J.M., Doyle, P., Janssen, N., Leng, M.J., Müller, W., Reboulet, S., 2013. Evaluating Mg/Ca in belemnite calcite as a palaeo-proxy. *Palaeogeography, Palaeoclimatology, Palaeoecology* 388, 98-108.

Macquaker, J.H.S. 1994. A lithofacies study of the Peterborough Member, Oxford Clay Formation (Jurassic), UK: an example of sediment bypass in a mudstone succession. *Journal of the Geological Society, London* 151, 161-172.

Martill, D.M., Taylor, M.A., Duff, K.L., Riding, J.B., Bown., P.R., 1994. The trophic structure of the biota of the Peterborough Member, Oxford Clay Formation (Jurassic), UK. *Journal of the Geological Society, London* 151, 173-194.

McArthur, J.M., Doyle, P., Leng, M.J., Reeves, K., Williams, C.T., Garcia-Sanchez, R., Howarth, R.J., 2007. Testing Palaeo-environmental proxies in Jurassic belemnites: Mg/Ca, Sr/Ca, Na/Ca,  $\delta^{18}\text{O}$  and  $\delta^{13}\text{C}$ . *Palaeogeography, Palaeoclimatology, Palaeoecology* 252, 464-480.

Morgans, H.S., 1999. Lower and middle Jurassic woods of the Cleveland Basin (North Yorkshire), England. *Palaeontology* 42, 303-326.

Morgans, H.S., Hesselbo, S.P., Spicer, R.A., 1999. The seasonal climate of Early-Middle Jurassic, Cleveland Basin, England. *Palios* 14, 261-272.

Mutterlose, J., Malkoc, M., Schouten, S., Damsté, J.S.S., 2012. Reconstruction of vertical temperature gradients in past oceans — Proxy data from the Hauterivian–early Barremian (Early Cretaceous) of the Boreal Realm. *Palaeogeography, Palaeoclimatology, Palaeoecology* 363–364, 135–143.

Mutterlose, J., Malkoc, M., Schouten, S., Damsté, J.S.S., Forster, A., 2010. TEX<sub>86</sub> and stable  $\delta^{18}\text{O}$  paleothermometry of early Cretaceous sediments: Implications for belemnite ecology and paleotemperature proxy application. *Earth and Planetary Science Letters* 298, 286–298.

NOAA., 2009. World Ocean Atlas. [Online]. Available at:

[http://www.nodc.noaa.gov/OC5/WOA09F/pr\\_woa09f.html](http://www.nodc.noaa.gov/OC5/WOA09F/pr_woa09f.html)

Norry, M.J., Dunham, A.C., Hudson, J.D., 1994. Mineralogy and geochemistry of the Peterborough Member, Oxford Clay Formation, Jurassic, UK: element fractionation during mudrock sedimentation. *Journal of the Geological Society, London* 151, 195-207.

Nunn, E.V., Price, G.D., 2010. Late Jurassic (Kimmeridgian–Tithonian) stable isotopes ( $\delta^{18}\text{O}$ ,  $\delta^{13}\text{C}$ ) and Mg/Ca ratios: new palaeoclimate data from Helmsdale, northeast Scotland.

Palaeogeography, Palaeoclimatology, Palaeoecology 292, 325-335.

Nunn, E.V., Price, G.D., Hart, M.B., Page, K.N., Leng, M. J., 2009. Isotopic signals from Callovian–Kimmeridgian (Middle–Upper Jurassic) belemnites and bulk organic carbon, Staffin Bay, Isle of Skye, Scotland. Journal of the Geological Society 166, 633-641.

O'Neill, B.R., Manger, W.L., Hays, P.D., 2003. Growth and diagenesis of Middle Jurassic belemnite rostra from northeastern Utah: insights using cathodoluminescence, in: Warnke, K., Keupp, H., Boletzky, S.v., (Eds) Coleoid cephalopods through time, Berlin.

Page, K.N., 1989. A stratigraphical revision for the English Lower Callovian. Proceedings of the Geologists' Association 100, 363-382.

Pierre, C., 1999. The oxygen and carbon isotope distribution in the Mediterranean water masses. Marine Geology 153, 41-55.

Poulsen, N.E., Riding, J.B., 2003. The Jurassic dinoflagellate cyst zonation of Subboreal Northwest Europe. Geological Survey of Denmark and Greenland Bulletin 1, 115 – 144.

Price, G. D., 2010. Carbon-isotope stratigraphy and temperature change during the Early-Middle Jurassic (Toarcian-Aalenian), Raasay, Scotland. UK. Palaeogeography, Palaeoclimatology, Palaeoecology 285, 255-263.

Price, G.D., Fozy, I., Janssen, N.M.M. & Palfy, J., 2011. Late Valanginian-Barremian (Early Cretaceous) palaeotemperatures inferred from belemnite stable isotope and Mg/Ca ratios from Bersek Quarry (Gerecse Mountains, Transdanubian Range, Hungary). Palaeogeography, Palaeoclimatology, Palaeoecology 305, 1-9.

Price, G.D., Nunn, E.V., 2010. Valanginian isotope variation in glendonites and belemnites from Arctic Svalbard: Transient glacial temperatures during the Cretaceous greenhouse. Geology 38, 251-254.

Price, G.D., Mutterlose, J., 2004. Isotopic signals from late Jurassic-early Cretaceous (Volgian-Valanginian) sub-Arctic belemnites, Yatria River, Western Siberia. Journal of the Geological Society, London 161, 959-968.

Price, G.D., Page, K.N., 2008. A carbon and oxygen isotope analysis of molluscan faunas from the Callovian-Oxfordian boundary at Redcliffe Point, Weymouth, Dorset: implications for belemnite behaviour. *Proceedings of the Geologists' Association* 119, 153-160.

Price, G.D., Ruffell, A.H., Jones, C E., Kalin, R. M., Mutterlose, J., 2000. Isotopic evidence for temperature variation during the early Cretaceous (late Ryazanian-mid-Hauterivian). *Journal of the Geological Society, London* 157, 335-343.

Price, G.D., Rogov, M.A., 2009. An isotopic appraisal of the Late Jurassic greenhouse phase in the Russian Platform. *Palaeogeography, Palaeoclimatology, Palaeoecology* 273, 41-49.

Price, G.D., Sellwood, B.W., 1997. "Warm" palaeotemperatures from high Late Jurassic palaeolatitudes (Falkland Plateau): Ecological, environmental or diagenetic controls? *Palaeogeography, Palaeoclimatology, Palaeoecology* 129, 315-327.

Price, G.D., Williamson, T., Henderson, RA., Gagan, MK., 2012. Barremian-Cenomanian palaeotemperatures for Australian seas based on new oxygen-isotope data from belemnite rostra. *Palaeogeography, Palaeoclimatology, Palaeoecology* 358, 27-39.

Rexfort, A., Mutterlose, J., 2006. Stable isotope records from *Sepia officinalis* – a key to understanding the ecology of belemnites. *Earth and Planetary Science Letters* 247, 212 – 221.

Rosales, I., Quesada, S., Robles, S., 2001. Primary and diagenetic isotopic signals in fossils and hemipelagic carbonates. The Lower Jurassic of northern Spain. *Sedimentology* 48, 1149-1169.

Rosales, I., Robles, S., Quesada, S., 2004. Elemental and oxygen isotope composition of early Jurassic belemnites: salinity vs. temperature signals. *Journal of Sedimentary Research* 74, 342-354.

Scheurle, C., Hebbeln, D., 2003. Stable oxygen isotopes as recorders of salinity and river discharge in the German Bight, North Sea. *Geo-Mar Letters* 23, 130–136

Schöne, B.R., Fiebig, J., Pfeiffer, M., Gleß, R., Hickson, J., Johnson, A.L.A., Dreyer, W., Oschmann, W., 2005. Climate records from a bivalved Methuselah (*Arctica islandica*, Mollusca; Iceland). *Palaeogeography, Palaeoclimatology, Palaeoecology* 228, 130-148.

Schöne, B.R., Wanamaker, A.D., Fiebig, J., Thébault, J., Kreutz, K., 2011. Annually resolved  $\delta^{13}\text{C}$  shell chronologies of long-lived bivalve mollusks (*Arctica islandica*) reveal oceanic carbon dynamics in the temperate North Atlantic during recent centuries. *Palaeogeography, Palaeoclimatology, Palaeoecology* 302, 31-42.

Sellwood, B.W., Valdes, P.J., 1997. Geological evaluation of climate General Circulation Models and model implications for Mesozoic cloud cover. *Terra Nova* 9, 75 – 78.

Steuber, T., 1999. Isotopic and chemical intra-shell variations in low-Mg calcite of rudist bivalves (Mollusca-Hippuritacea): disequilibrium fractionations and late Cretaceous seasonality. *International Journal of Earth Sciences* 88, 551-570.

Thiery, J. Guiraud, R., 2000. Middle Toarcian, in: Dercourt, J., Gaetani, M., Vrielynck, B., Barrier, E., Biju-Duval, B., Brunet, M.-F., Cadet, J.P., Crasquin, S., Sandulescu, M. (Eds.), *Atlas of peri-Tethys palaeogeographical maps, vol. I-XX.CCGM/CGMW, Paris, map 8, (40 co-authors).*

Tomašových, A., Farkaš, J., 2005. Cathodoluminescence of Late Triassic terabratulid brachiopods: implications for growth patterns. *Palaeogeography, Palaeoclimatology, Palaeoecology* 216, 215-233.

Voigt, S., Wilmsen, M., Mortimore, R.N., Voigt, T., 2003. Cenomanian palaeotemperatures derived from the oxygen isotopic composition of brachiopods and belemnites: evaluation of Cretaceous palaeotemperature proxies. *International Journal of Earth Sciences* 92, 285-299.

Wierzbowski, H., 2004. Carbon and oxygen isotope composition of Oxfordian-Early Kimmeridgian belemnite rostra: palaeoenvironmental implications for Late Jurassic seas. *Palaeogeography, Palaeoclimatology, Palaeoecology* 203, 153-168.

Wierzbowski, H., Joachimski, M.M., 2007. Reconstruction of late Bajocian–Bathonian marine palaeoenvironments using carbon and oxygen isotope ratios of calcareous fossils from the Polish Jura Chain (central Poland). *Palaeogeography, Palaeoclimatology, Palaeoecology* 254, 523-540.

Wierzbowski, H., Joachimski, M.M., 2009. Stable isotopes, elemental distribution, and growth rings of belemnopsid belemnite rostra: Proxies for belemnite life habitat. *Palaios* 24, 377-386.

Wierzbowski, H., Dembicz, K., Praszker, T., 2009. Oxygen and carbon isotope composition of Callovian-Lower Oxfordian (Middle-Upper Jurassic) belemnite rostra from central Poland: a record of a Late Callovian global sea-level? *Palaeogeography, Palaeoclimatology, Palaeoecology* 283, 182-194.

Wilby, P.R., Hudson, J.D., Clements, R.G., Hollingworth, N.T.J., 2004. Taphonomy and origin of an accumulate of soft-bodied cephalopods in the Oxford Clay Formation (Jurassic, England). *Palaeontology* 47, 1159-1180.

Žák, K., Košťák, M., Otakar, M., Zakharov, V.A., Rogov, M.A., Pruner, P., Rohovec, J., Dzyuba, O.S., Mazuch, M., 2011. Comparison of carbonate C and O stable isotope records across the Jurassic/Cretaceous boundary in the Tethyan and Boreal Realms. *Palaeogeography, Palaeoclimatology, Palaeoecology* 299, 83-96.

Ziegler, P.A., 1990. *Geological Atlas of Western and Central Europe*. Shell International Petroleum, Maatschappij.

**Fig. 1. Outcrops of the Oxford Clay in England and specimen collection site.**

Map modified after Hudson and Martill (1994), areas of outcrop shown by shaded area and asterisk indicating site of collection

**Fig. 2. The Palaeogeography of North-West Europe in the Callovian**

Palaeogeographic map modified after Bradshaw et al. (1992), asterisk indicates site of collection of specimens

**Fig. 3. Stratigraphy of the lower part of the Peterborough Member in the Peterborough area.**

Diagram modified after Hudson and Martill (1994b).

**Fig. 4. Sampling of *G. (B.) dilobotes* and measurement of distance from umbo**

**Fig. 5. Sampling of *C. puzosiana***

(A, position from which slabs were cut. B, how samples were milled in relation to age)

**Fig.6. Through ontogeny  $\delta^{18}\text{O}$  and  $\delta^{13}\text{C}$  for *G. (B.) dilobotes* and *C. puzosiana***

**Table 1. Isotope data for specimens of *G. (B.) dilobotes***

**Table 2. Isotope data for specimens of *C. puzosiana***

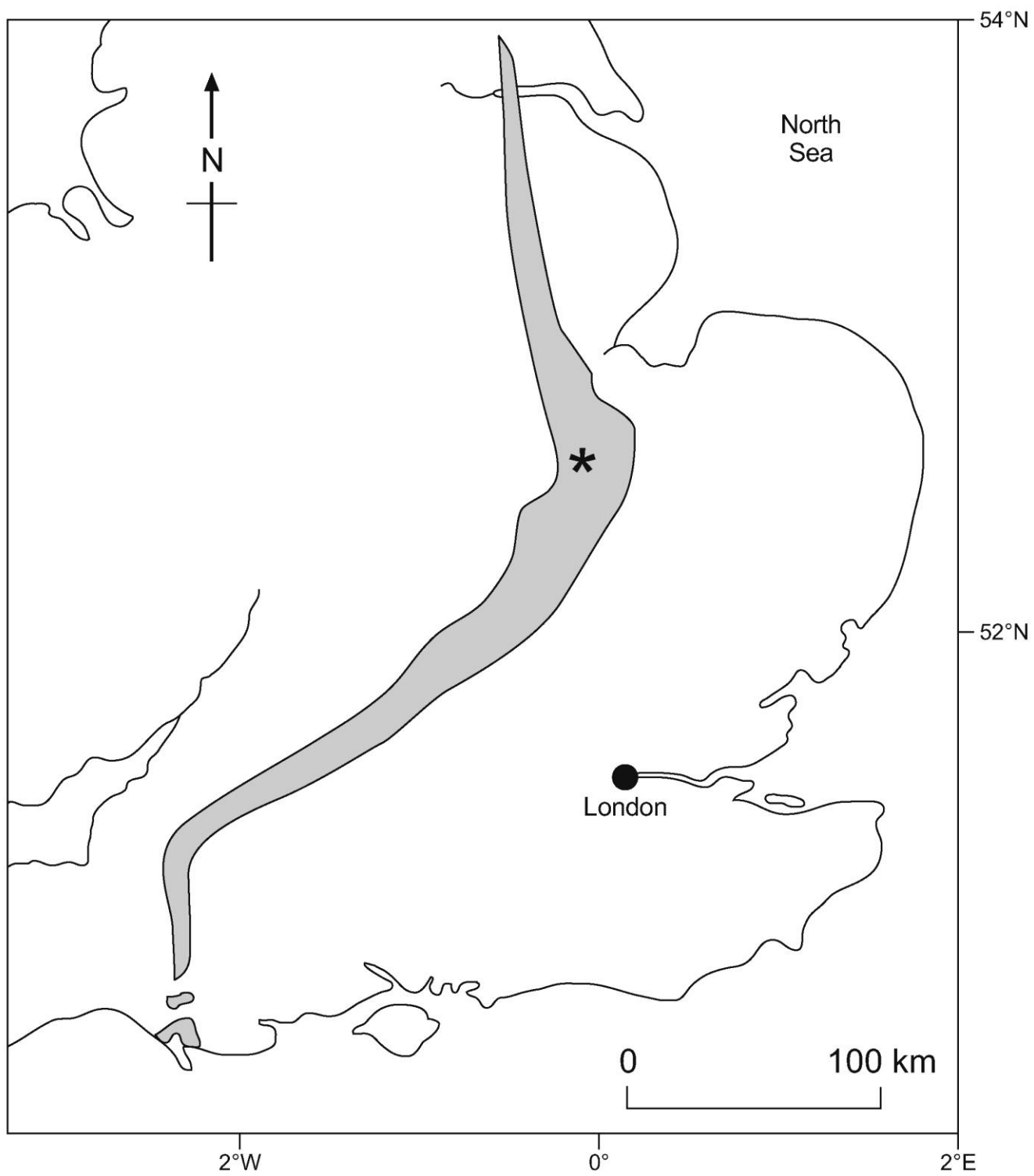


Figure 1

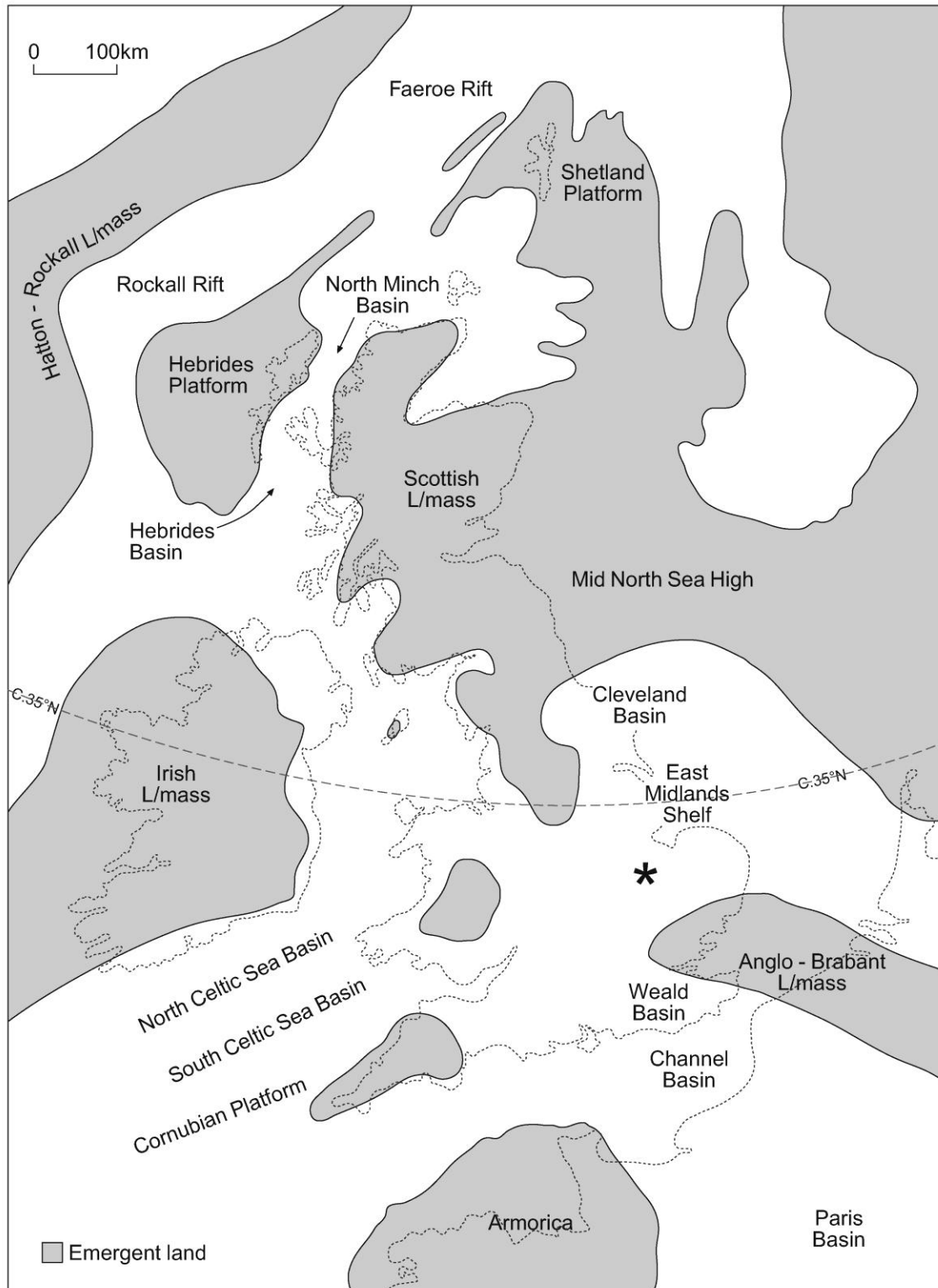


Figure 2

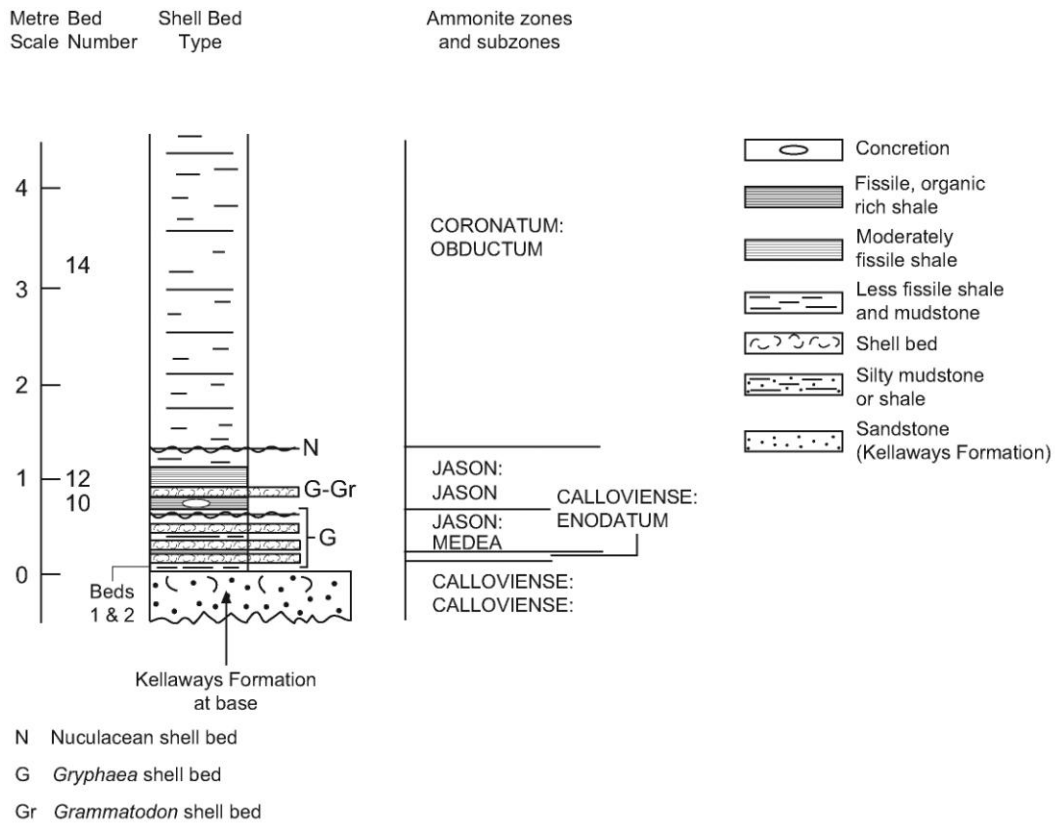


Figure 3

ACCEPTED

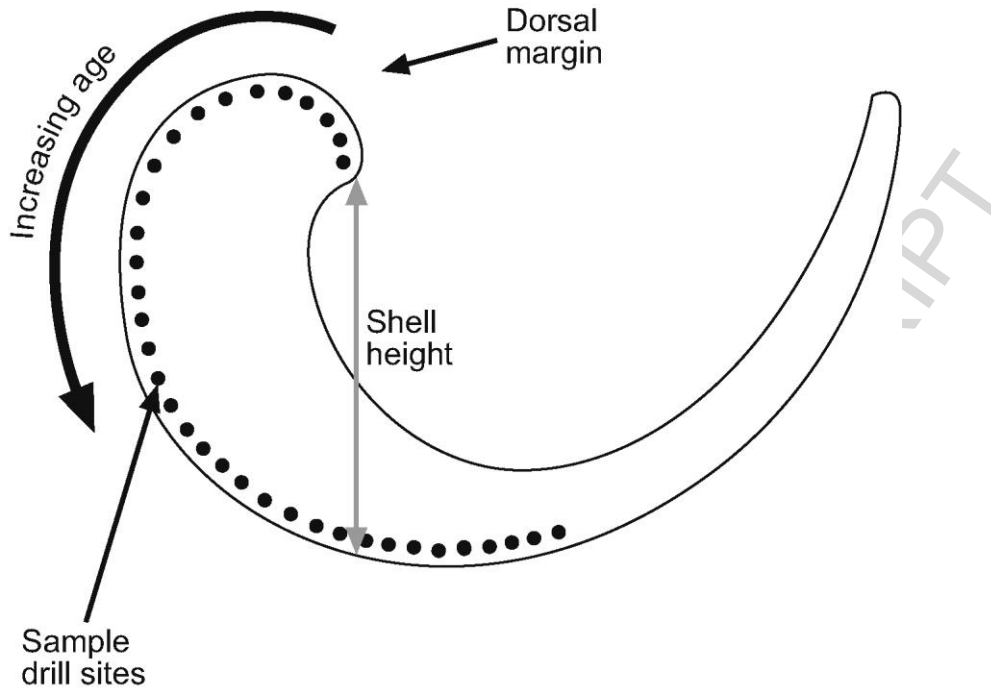


Figure 4

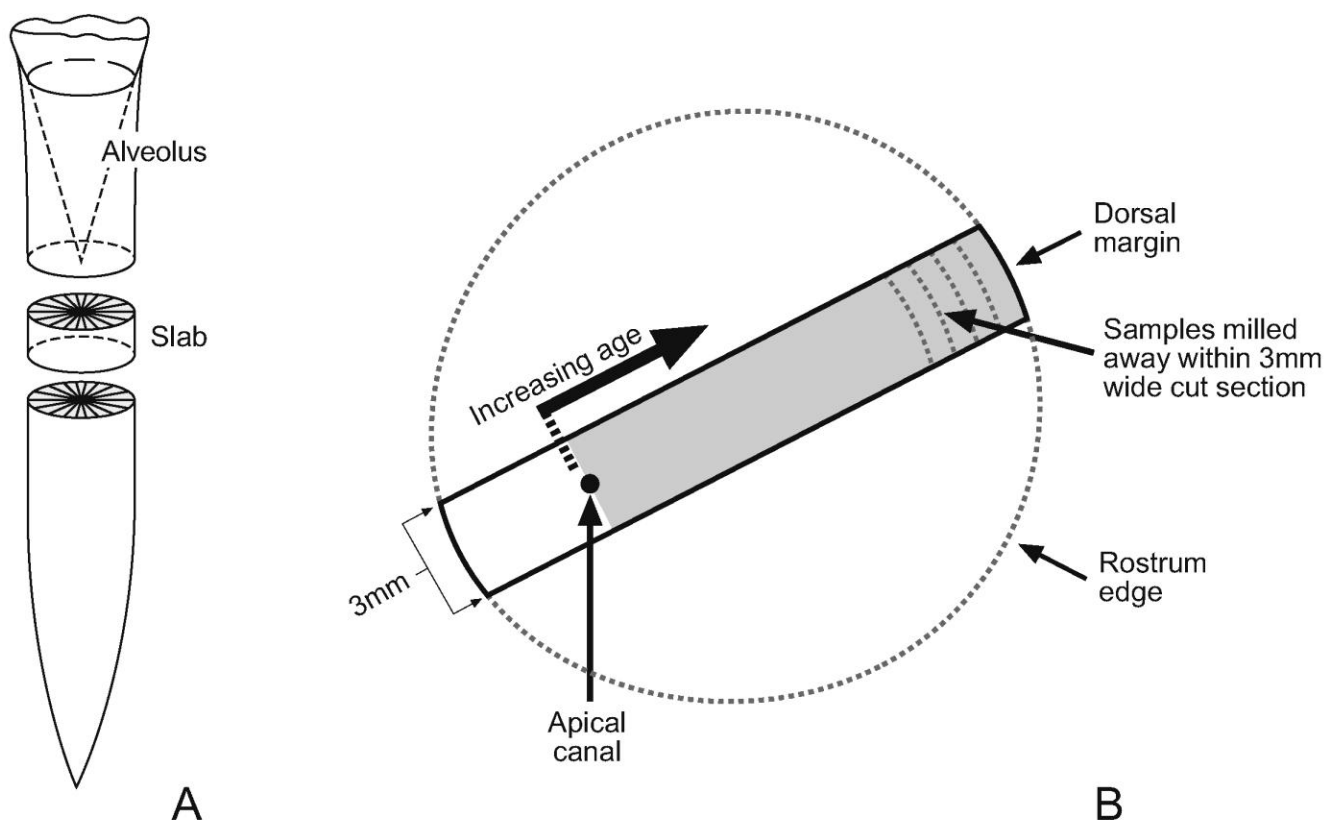


Figure 5

ACCEPTED

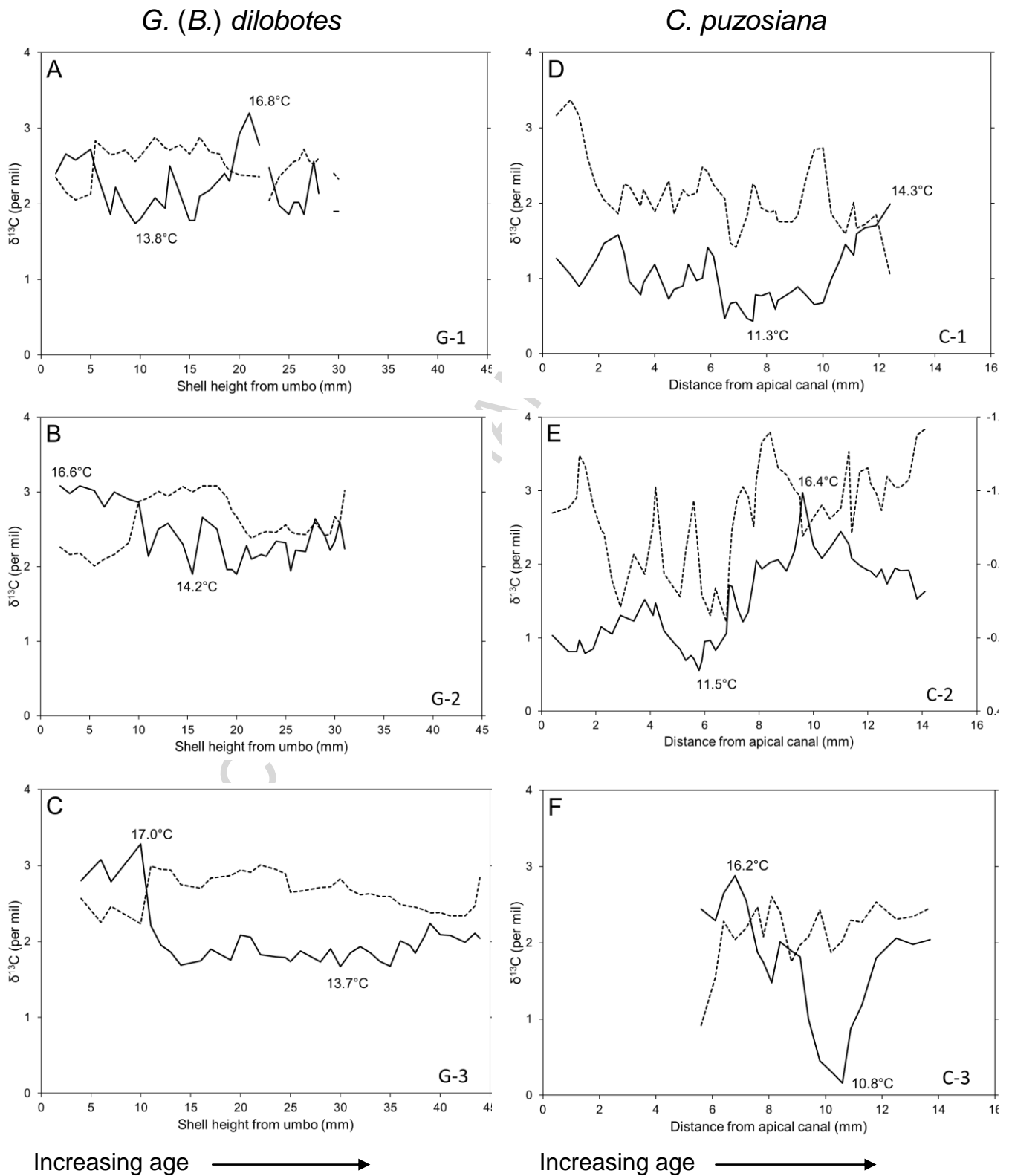


Fig. 6. Incremental stable isotope data for Callovian specimens of *G. (B.) dilobotes* (6a) – (6c) and *C. puzosiana* (6d) – (6f). Oxygen isotope data is shown by a solid line and carbon isotope

data by a dashed line. Note that the oxygen isotope axis is reversed in order that more depleted values of  $\delta^{18}\text{O}$ , indicating warmer temperatures, plot towards the top.

ACCEPTED MANUSCRIPT

Table 1 Incremental stable isotope data for specimens of *G. (B.) dilobotes*.

Sample number	Distance from umbo (mm) <sup>a</sup>	$\delta^{13}\text{C}$ (‰)	$\delta^{18}\text{O}$ (‰)	Sample number	Distance from umbo (mm) <sup>a</sup>	$\delta^{13}\text{C}$ (‰)	$\delta^{18}\text{O}$ (‰)
<b>UoD55368 – G1</b>				<b>UoD55369 – G2 (cont.)</b>			
G1 - 01	01.5	2.35	-0.80	G2 - 17	19.5	2.74	-0.58
G1 - 02	02.5	2.15	-0.93	G2 - 18	20.0	2.67	-0.55
G1 - 03	03.5	2.05	-0.89	G2 - 19	21.0	2.45	-0.74
G1 - 04	05.0	2.13	-0.96	G2 - 20	21.5	2.38	-0.65
G1 - 05	05.5	2.83	-0.83	G2 - 21	22.5	2.45	-0.68
G1 - 06	07.0	2.65	-0.53	G2 - 22	23.0	2.47	-0.67
G1 - 07	07.5	2.66	-0.71	G2 - 23	24.0	2.46	-0.77
G1 - 08	08.5	2.71	-0.57	G2 - 24	25.0	2.56	-0.76
G1 - 09	09.5	2.56	-0.47	G2 - 25	25.5	2.47	-0.57
G1 - 10	10.0	2.63	-0.50	G2 - 26	26.0	2.44	-0.71
G1 - 11	11.5	2.88	-0.64	G2 - 27	27.0	2.43	-0.70
G1 - 12	12.5	2.74	-0.57	G2 - 28	28.0	2.59	-0.92
G1 - 13	13.0	2.71	-0.85	G2 - 29	29.0	2.42	-0.80
G1 - 14	14.0	2.78	-0.67	G2 - 30	29.5	2.43	-0.71
G1 - 15	15.0	2.66	-0.49	G2 - 31	30.0	2.67	-0.77
G1 - 16	15.5	2.75	-0.49	G2 - 32	30.5	2.59	-0.90
G1 - 17	16.0	2.88	-0.65	G2 - 33	31.0	3.02	-0.72
G1 - 18	17.0	2.69	-0.69				
G1 - 19	18.0	2.66	-0.76	<b>UoD55370 –G3</b>			
G1 - 20	18.5	2.52	-0.80	G3 - 01	04.0	2.57	-1.00
G1 - 21	19.0	2.44	-0.75	G3 - 02	06.0	2.25	-1.14
G1 - 22	20.0	2.38	-1.06	G3 - 03	07.0	2.46	-0.99
G1 - 23	21.0	2.37	-1.20	G3 - 04	10.0	2.23	-1.24
G1 - 24	22.0	2.36	-0.99	G3 - 05	11.0	2.99	-0.70
G1 - 25 <sup>b</sup>	22.5	0.80	-6.20	G3 - 06	12.0	2.95	-0.57
G1 - 26	23.0	2.04	-0.84	G3 - 07	13.0	2.94	-0.53
G1 - 27	24.0	2.36	-0.59	G3 - 08	14.0	2.75	-0.44
G1 - 28	25.0	2.49	-0.53	G3 - 09	16.0	2.70	-0.47
G1 - 29	25.5	2.56	-0.61	G3 - 10	17.0	2.84	-0.55
G1 - 30	26.0	2.58	-0.61	G3 - 11	19.0	2.87	-0.48
G1 - 31	26.5	2.72	-0.53	G3 - 12	20.0	2.94	-0.64
G1 - 32	27.0	2.57	-0.72	G3 - 13	21.0	2.91	-0.63
G1 - 33	27.5	2.52	-0.88	G3 - 14	22.0	3.01	-0.51
G1 - 34	28.0	2.60	-0.67	G3 - 15	23.5	2.95	-0.50
G1 - 35 <sup>b</sup>	28.5	1.20	-4.54	G3 - 16	24.5	2.89	-0.49
G1 - 36 <sup>c</sup>	29.0			G3 - 17	25.0	2.65	-0.47
G1 - 37	29.5	2.40	-0.55	G3 - 18	26.0	2.66	-0.54
G1 - 38	30.0	2.33	-0.55	G3 - 19	28.0	2.71	-0.46
				G3 - 20	29.0	2.72	-0.55
<b>UoD55369 – G2</b>				G3 - 21	30.0	2.82	-0.44
G2 - 01	02.0	2.26	-1.14	G3 - 22	31.0	2.68	-0.53
G2 - 02	03.0	2.16	-1.09	G3 - 23	32.0	2.62	-0.57
G2 - 03	04.0	2.18	-1.14	G3 - 24	33.0	2.63	-0.53
G2 - 04	05.5	2.01	-1.11	G3 - 25	34.0	2.59	-0.47
G2 - 05	06.5	2.10	-1.00	G3 - 26	35.0	2.59	-0.44
G2 - 06	07.5	2.16	-1.10	G3 - 27	36.0	2.48	-0.60
G2 - 07	09.0	2.32	-1.05	G3 - 28	37.0	2.46	-0.57
G2 - 08	10.0	2.87	-1.03	G3 - 29	37.5	2.45	-0.52
G2 - 09	11.0	2.92	-0.67	G3 - 30	38.5	2.41	-0.65
G2 - 10	12.0	3.01	-0.85	G3 - 31	39.0	2.38	-0.72
G2 - 11	13.0	2.94	-0.89	G3 - 32	40.0	2.38	-0.64
G2 - 12	14.5	3.07	-0.75	G3 - 33	41.0	2.34	-0.64
G2 - 13	15.5	3.00	-0.55	G3 - 34	42.5	2.34	-0.60
G2 - 14	16.5	3.08	-0.93	G3 - 35	43.5	2.47	-0.65
G2 - 15	18.0	3.08	-0.85	G3 - 36	44.0	2.85	-0.62
G2 - 16	19.0	2.93	-0.58				

<sup>a</sup> Rounded to nearest 0.5 mm<sup>b</sup> Data excluded from further analysis – altered portion of specimen<sup>c</sup> Technical problem recovering data

Table 2 Incremental stable isotope data for specimens of *C. puzosiana*.

Sample number	Distance from apical canal (mm) <sup>a</sup>	$\delta^{13}\text{C}$ (‰)	$\delta^{18}\text{O}$ (‰)	Sample number	Distance from apical canal (mm) <sup>a</sup>	$\delta^{13}\text{C}$ (‰)	$\delta^{18}\text{O}$ (‰)
<b>UoD55371 – C1</b>				<b>UoD55372 – C2 (cont.)</b>			
C1 - 01	0.6	3.17	-0.23	C2 - 19	5.5	2.63	0.02
C1 - 02	1.0	3.37	-0.12	C2 - 20	5.6	2.87	0.04
C1 - 03	1.3	3.16	-0.05	C2 - 21	5.8	2.03	0.12
C1 - 04	1.6	2.60	-0.13	C2 - 22	5.9	1.57	0.06
C1 - 05	1.9	2.24	-0.22	C2 - 23	6.0	1.50	-0.08
C1 - 06	2.2	2.04	-0.33	C2 - 24	6.2	1.30	-0.08
C1 - 07	2.7	1.86	-0.39	C2 - 25	6.4	1.68	-0.02
C1 - 08	2.9	2.25	-0.27	C2 - 26	6.5	1.54	-0.04
C1 - 09	3.1	2.22	-0.08	C2 - 27	6.8	1.21	-0.13
C1 - 10	3.5	1.96	0.01	C2 - 28	6.9	1.97	-0.46
C1 - 11	3.6	2.18	-0.07	C2 - 29	7.0	2.47	-0.45
C1 - 12	4.0	1.88	-0.19	C2 - 30	7.2	2.89	-0.30
C1 - 13	4.5	2.29	0.04	C2 - 31	7.4	3.05	-0.21
C1 - 14	4.7	1.86	-0.03	C2 - 32	7.6	2.92	-0.27
C1 - 15	5.0	2.18	-0.05	C2 - 33	7.8	2.51	-0.50
C1 - 16	5.2	2.10	-0.19	C2 - 34	7.9	3.14	-0.63
C1 - 17	5.5	2.13	-0.09	C2 - 35	8.1	3.66	-0.57
C1 - 18	5.7	2.48	-0.10	C2 - 36	8.4	3.80	-0.61
C1 - 19	5.9	2.42	-0.31	C2 - 37	8.7	3.32	-0.63
C1 - 20	6.1	2.25	-0.25	C2 - 38	9.0	3.22	-0.55
C1 - 21	6.5	2.06	0.17	C2 - 39	9.3	3.01	-0.69
C1 - 22	6.7	1.47	0.07	C2 - 40	9.5	2.93	-0.90
C1 - 23	6.9	1.42	0.06	C2 - 41	9.7	2.38	-1.09
C1 - 24	7.3	1.84	0.17	C2 - 42	10.0	2.64	-0.73
C1 - 25	7.5	2.26	0.18	C2 - 43	10.3	2.80	-0.64
C1 - 26	7.6	2.21	0.01	C2 - 44	10.6	2.62	-0.71
C1 - 27	7.8	1.93	0.02	C2 - 45	11.0	2.76	-0.82
C1 - 28	8.1	1.87	0.00	C2 - 46	11.3	3.53	-0.73
C1 - 29	8.3	1.90	0.11	C2 - 47	11.4	2.42	-0.64
C1 - 30	8.4	1.75	0.05	C2 - 48	11.7	3.26	-0.59
C1 - 31	8.9	1.75	-0.01	C2 - 49	12.0	3.31	-0.56
C1 - 32	9.1	1.83	-0.04	C2 - 50	12.1	3.10	-0.55
C1 - 33	9.4	2.32	0.01	C2 - 51	12.3	2.96	-0.51
C1 - 34	9.7	2.71	0.07	C2 - 52	12.5	2.73	-0.57
C1 - 35	10.0	2.73	0.06	C2 - 53	12.7	3.19	-0.46
C1 - 36	10.4	1.86	-0.10	C2 - 54	13.0	3.05	-0.57
C1 - 37	10.6	1.70	-0.22	C2 - 55	13.2	3.05	-0.56
C1 - 38	10.8	1.59	-0.33	C2 - 56	13.5	3.15	-0.56
C1 - 39	11.1	2.01	-0.25	C2 - 57	13.8	3.76	-0.36
C1 - 40	11.2	1.67	-0.40	C2 - 58	14.1	3.84	-0.42
C1 - 41	11.5	1.72	-0.44				
C1 - 42	12.0	1.84	-0.45	<b>UoD55373 –C3</b>			
C1 - 43	12.3	1.04	-0.59	C3 - 01	5.6 <sup>b</sup>	0.92	-0.82
				C3 - 02	6.1	1.55	-0.75
				C3 - 03	6.4	2.28	-0.92
				C3 - 04	6.8	2.04	-1.04
				C3 - 05	7.2	2.19	-0.87
				C3 - 06	7.6	2.47	-0.54
				C3 - 07	7.8	2.08	-0.47
				C3 - 08	8.1	2.61	-0.34
				C3 - 09	8.4	2.41	-0.61
				C3 - 10	8.8	1.75	-0.55
				C3 - 11	9.1	1.97	-0.51
				C3 - 12	9.4	2.08	-0.10
				C3 - 13	9.8	2.43	0.17
				C3 - 14	10.2	1.87	0.24
				C3 - 15	10.6	2.03	0.32
				C3 - 16	10.9	2.29	-0.04
				C3 - 17	11.3	2.27	-0.19
				C3 - 18	11.8	2.53	-0.50
<b>UoD55372 – C2</b>							
C2 - 01	0.4	2.70	-0.12				
C2 - 02	1.0	2.76	-0.01				
C2 - 03	1.3	2.90	-0.01				
C2 - 04	1.4	3.48	-0.09				
C2 - 05	1.6	3.34	0.01				
C2 - 06	1.9	2.81	-0.03				
C2 - 07	2.2	2.46	-0.18				
C2 - 08	2.3	2.42	-0.16				
C2 - 09	2.6	1.78	-0.13				
C2 - 10	2.9	1.42	-0.25				
C2 - 11	3.4	2.13	-0.21				
C2 - 12	3.8	1.86	-0.36				
C2 - 13	4.1	2.52	-0.25				
C2 - 14	4.2	3.05	-0.34				
C2 - 15	4.5	1.87	-0.15				

C2 - 16	4.9	1.66	-0.06	C3 - 19	12.5	2.31	-0.63
C2 - 17	5.1	1.56	-0.02	C3 - 20	13.1	2.34	-0.59
C2 - 18	5.3	2.19	0.06	C3 - 21	13.7	2.46	-0.62

<sup>a</sup> Distance from apical canal rounded to nearest 0.1 mm

<sup>b</sup> Areas closer to apical canal than 5.5mm not sampled

ACCEPTED MANUSCRIPT

**Highlights**

- $\delta^{18}\text{O}$  signals from *G. (B.) dilobotes* reveal Callovian seasonality in UK benthic waters
- Depth of UK Callovian seas in the collection locality estimated to be 50m
- Incremental  $\delta^{18}\text{O}$  signals from *C. puzosiana* suggest migratory lifestyle for this species

ACCEPTED MANUSCRIPT